University of Alberta

Examination of Protein Adsorption with Surface Sensitive Spectroscopic Techniques

By

Francis Nsiah

A thesis submitted to the Faculty of Graduate Studies and Research in partial fulfillment of the requirements for the degree of Master of Science

Department of Chemistry

Edmonton, Alberta

Spring 2003

National Library of Canada
Acquisitions and Bibliographic Services
395 Wellington Street
Ottawa ON K1A 0N4
Canada

Bibliothèque nationale du Canada
Acquisitions et services bibliographiques
395, rue Wellington
Ottawa ON K1A 0N4
Canada

Your file Votre référence

Our file Notre référence

The author has granted a non-exclusive licence allowing the National Library of Canada to reproduce, loan, distribute or sell copies of this thesis in microform, paper or electronic formats.

L'auteur a accordé une licence non exclusive permettant à la Bibliothèque nationale du Canada de reproduire, prêter, distribuer ou vendre des copies de cette thèse sous la forme de microfiche/film, de reproduction sur papier ou sur format électronique.

The author retains ownership of the copyright in this thesis. Neither the thesis nor substantial extracts from it may be printed or otherwise reproduced without the author's permission.

L'auteur conserve la propriété du droit d'auteur qui protège cette thèse. Ni la thèse ni des extraits substantiels de celle-ci ne doivent être imprimés ou autrement reproduits sans son autorisation.

0-612-82321-0

Canada

University of Alberta

Library Release Form

Name of Author: Francis Nsiah

Title of Thesis: Examination of Protein Adsorption with Surface Sensitive Spectroscopic Techniques

Degree: Master of Science

Year this Degree Granted: 2003

Permission is hereby granted to the University of Alberta Library to reproduce single copies of this thesis and to lend or sell such copies for private, scholarly or scientific research purposes only.

The author reserves all other publication and other rights in association with the copyright in the thesis, and except as herein before provided, neither the thesis nor any substantial portion thereof may be printed or otherwise reproduced in any material form whatever without the author's prior written permission.

607E Michener Park
Edmonton, Alberta
Canada T6H 5A1

March 28, 2003

University of Alberta

Faculty of Graduate Studies and Research

The undersigned certify that they have read, and recommended to the Faculty of Graduate Studies and Research for acceptance, a thesis entitled "Examination of Protein Adsorption with Surface Sensitive Spectroscopic Techniques" submitted by Francis Nsiah in partial fulfillment of the requirements for the degree of Master of Science in Chemistry.

Dr. Mark T. McDermott

Dr. Hasan Uludag

Dr. John-Bruce Green
Committee Chair and Examiner,
University of Alberta

27-MARCH-2003
Date

The road to success is always under construction but without goals the routines of life become the rusts of life... He who wishes to eat the nut does not mind cracking the shell.

Unknown

ABSTRACT

The ability to control specific and non-specific protein adsorption at solid interfaces is a key to the design of implant materials, biosensors, and improved separation techniques. One of the major difficulties has been in the determination of the conformation and/or orientation of adsorbed protein on different surfaces. In this thesis, infrared reflection absorption spectroscopy (IRRAS) and surface plasmon resonance (SPR) imaging were employed to explore adsorption characteristics of human fibrinogen (HFG) human fibronectin (HFN), bovine serum albumin (BSA) and lysozyme (LYS).

Self-assembled monolayers (SAMs) on gold were used to control surface chemistry. The SAMs were characterized using IRRAS and contact angle measurements. Octadecanethiol (ODT) was used as a model neutral, hydrophobic surface. 16-mercapto-hexadecanoic acid (MHA) provides a hydrophilic, partially negatively charged surface at pH 7.4. CH_2OH terminated monolayers of 11-mercapto-1-undecanol (MUL) was employed as a protein-resistant control surface. The differences in chemistries of the SAMs provided a platform to map variations in the amount of protein adsorbed and surface-induced protein conformation and/or orientation.

IRRAS was employed on single component monolayers to obtain information on surface coverage as well as on the adsorbed state of the proteins. Comparison of amide I band positions of the adsorbed proteins to their native

protein samples was used to probe deviations from their native conformations dictated by surface chemistry. Peak intensities of the amide II bands were used to track the amount o protein adsorbed to each surface. Both HFG and HFN showed similar amide II peak heights on ODT and MHA surfaces indicating that both proteins adsorb in similar amounts to CH_3 and COOH terminated surfaces. Antibody binding to HFG demonstrated that fibrinogen adsorbs in distinct states on methyl and carboxylic acid terminated monolayers.

SPR imaging has been used for the first time as a means to visualized adsorbed state of proteins on patterned substrates. Chemically patterned monolayer surfaces were created using microcontact printing technique. Differences in image contrast were attributed to differences in the state of the adsorbed protein. Antibody binding and surfactant elution studies will be described to further substantiate this claim. Overall, we have been able to establish using both IRRAS and SPR imaging techniques that surface chemistry influences the adsorption characteristics of proteins. In addition, SPR imaging was shown to be a versatile tool capable of providing differences in protein adsorption on patterned surfaces not obtainable via other surface sensitive spectroscopic techniques.

ACKNOWLEDGEMENTS

To God be the glory for great things He has done. I am also greatly indebted to several people who have contributed immensely in diverse ways to my academic career and especially towards the preparation of this thesis.

First of all, I wish to express my sincere appreciation to my M.Sc. supervisor, Dr. Mark McDermott for his guidance, advice and encouragement. Mark, your noble deeds will forever be remembered in time and in eternity. I remember very well your encouraging words during difficult moments. Indeed, you did not only act as a research director but also as a caring and concerned friend. I am indeed grateful to you Mark for your help throughout my stay in your group. It has been an enjoyable experience and a time well spent. In a nutshell, I wish to thank you again for the confidence and trust you have reposed in me and to even welcome me back into your group for my Ph.D. program. God richly bless you for the good training and exposure to surface chemistry and protein studies.

I also wish to thank all the McDermott group members for their useful suggestions and even discussions outside chemistry. Thank you again for changing my name from Francis to Frank. I would like to also acknowledge the old group members, James, Truong, Gregory and Mirwais. Without your assistance this journey would not have been possible. Jimmy and Greg, your good advice and assistance will not be forgotten. I must also thank Vishal, Aaron, Solomon, Beatrice, Bushra, Chris, Abbas, Salome and Dwayne. Thank you all for the

togetherness, informative discussions and the conducive atmosphere you created towards this accomplishment.

Moreover, I am grateful to the Department of Chemistry for their financial support, the Faculty of Graduate Studies and Research and the Natural Science and Engineering Research Council of Canada (NSERC) for funding my research. I am indebted to my M.Sc. committee for their excellent and incisive comments on this thesis. In addition, I thank the entire faculty and the staff in the Chemistry Department especially Ilona and Dr. Cantwell. Thank you very much for your encouragement and precious advice.

It will be the greatest mistake ever, if I fail to acknowledge the immense contribution of my dear wife Comfort and my son Samuel. Connie, thank you for your patience, special love, and encouraging words offered throughout my studies. Samuel, I will forever remember your special smile that brings relief after hard day's toil. Thank you and I owe all of you a great deal. I also thank my mum who single handedly sponsored my education. Mum, may God richly reward you for your labour of love. I wish to say a big thank you to my family in Ghana, my in-laws, and all church members both in Ghana and in Edmonton for their support and prayers.

Finally, I wish to thank all the staff members at the Department of Chemistry (University of Cape Coast) and the teaching staff at the Mfantsipim School especially the headmaster, Mr. C. K. Eshun for their encouragement. I also thank my friends, Fred, Leonard, Stephen, Ademola, and Yaw Opoku for their

support, advice and encouragement. I know my acknowledgement list is incomplete. If I forgot to mention your name, please bear with me and accept my thanks.

Dedicated to my wife Comfort...
to my son Samuel...
and to my mother for her support and foresight.
Without these dear ones, this accomplishment would
not have been possible.

TABLE OF CONTENTS

CHAPTER I: INTRODUCTION	PAGE
Surface Interactions	1
Protein Adsorption at Interfaces	2
Protein Structure	2
Protein Adsorption	3
Plasma Proteins	8
Self-Assembled Monolayers	11
Research Objectives	16
References	17

CHAPTER II: PROBING PROTEIN ADSORPTION ON SELF-ASSEMBLED MONOLAYERS WITH INFRARED REFLECTION ABSORPTION SPECTROSCOPY

Introduction	22
Experimental	24
Results and Discussion	27
Conclusions	61
References	62

CHAPTER III: INVESTIGATION OF PROTEIN ADSORPTION ON PATTERNED SURFACES USING SURFACE PLASMON RESONANCE IMAGING

Introduction 67

Experimental 72

Results and Discussion 75

Conclusions 90

References 91

CHAPTER IV: CONCLUSIONS AND FUTURE WORKS

Overall Conclusions 95

Suggestions for Future Works 97

References 99

LIST OF TABLES

Table 1.1	Summary of the molecular weight, isoelectric point and charge at physiological pH of proteins of interest	9
Table 2.1	C-H stretching frequencies for ODT, MHA and MUL self-assembled monolayers on Au	29
Table 2.2	Advancing contact angle measurements of ODT, MHA, MUL, polystyrene and unmodified Au surfaces	32
Table 2.3	Spectroscopic of HFG on different substrates compared to those of its solid crystal	36
Table 2.4	Tabulated spectroscopic measurements for HFN	43
Table 2.5	Analysis of amide I and amide II bands for BSA	48
Table 2.6	Analysis of amide I and amide II bands for LYS	53
Table 2.7	Analysis of amide II peak intensities for anti-HFG and bIgG adsorbed to bound HFG on ODT and MHA modified Au substrates	59

LIST OF FIGURES

Figure 1.01	Schematic representation of adsorption of protein from solution onto a substrate.	5
Figure 1.02	Schematic representation of the chemisorption of the alkanethiol monolayers on Au(111) substrate.	14
Figure 2.01	FTIR spectrum of polystyrene on gold substrate.	30
Figure 2.02	IRRAS spectra for human fibrinogen (HFG) following 1 h adsorption time on surfaces with different chemistries.	35
Figure 2.03	Bar graph depicting amount of HFG adsorbed on different surface chemistries.	39
Figure 2.04	Spectra obtained by IRRAS of human fibronectin (HFN) after 1 h adsorption on different surfaces.	41
Figure 2.05	Bar graph showing the amide II band intensities of HFN on different substrates.	44
Figure 2.06	IRRAS spectra of bovine albumin (BSA) adsorbed on different substrates for 1 h.	47
Figure 2.07	Graphical representation of the amount of BSA adsorbed on different substrates depicted by amide II peak intensity.	49
Figure 2.08	IRRAS investigation of lysozyme (LYS) films adsorbed onto modified and unmodified Au/Ti/glass substrates.	52

Figure 2.09	Bar graph showing the amount of LYS on different substrates depicted by amide II peak intensity.	55
Figure 2.10	IRRAS investigation of HFG films adsorbed onto ODT and MHA modified Au surfaces, before and after exposure to anti-HFG and bovine IgG.	58
Figure 3.01	Schematic representation of the SPR biosensor.	70
Figure 3.02	Surface plasmon resonance imaging instrumental setup.	71
Figure 3.03	Adsorption of human fibrinogen (HFG) on ODT/MHA patterned monolayer surfaces.	77
Figure 3.04	SPR difference image showing HFG adsorption on ODT/MUL patterned Au substrate.	78
Figure 3.05	SPR difference images showing SDS elution of adsorbed HFG on ODT/MHA patterned gold substrates.	81
Figure 3.06	SPR difference images showing anti-HFG binding to HFG adsorbed to ODT/MHA patterned monolayers.	83
Figure 3.07	SPR difference images showing HFN adsorption on ODT/MHA and ODT/MUL patterned monolayer surfaces	85
Figure 3.08	SPR difference images showing SDS elution of adsorbed HFN on ODT/MHA patterned gold substrates.	87

Figure 3.09 SPR difference images showing anti-HFN binding to HFN adsorbed to ODT/MHA patterned monolayers. 89

LIST OF SYMBOLS

Å	A distance unit (angstroms)
A_{aI}	Absorbance value of amide I band
A_{aII}	Absorbance value of amide II band
θ_a	Advancing contact angle
θ	Angle of incidence
Ψ	Ellipsometric parameter
Δ	Ellipsometric parameter
A_{PAII}	Peak area of amide II band
n	Refractive index
ν_a	Wavenumber (cm^{-1}) for the asymmetric C-H stretch
ν_s	Wavenumber (cm^{-1}) for the symmetric C-H stretch
ν_{aI}	Wavenumber (cm^{-1}) of amide I band
ν_{aII}	Wavenumber (cm^{-1}) of amide II band

LIST OF ABBREVIATIONS

μCP	Microcontact printing
AFM	Atomic force microscopy
Ag	Silver
Anti-HFG	Antibody to human fibrinogen
Anti-HFN	Antibody to human fibronectin
Au	Gold
Au-SR	Gold-alkylthiolate bond
BAU	Unmodified gold
bIgG	Bovine immunoglobulin G
BSA	Bovine serum albumin
CCD	Charge coupled device
CD	Circular dichroism
Cr	Chromium
FTIR	Fourier transform infrared

FT-SPR	Fourier transform-surface plasmon resonance
HFG	Human fibrinogen
HFN	Human fibronectin
IgG	Immunoglobulin G
IR	Infrared
IRRAS	Infrared reflectance absorbance spectroscopy
LB	Langmuir-Blodgett
LYS	Lysozyme
MCT	Mercury-cadmium-telluride
MHA	Mercaptodecanoic acid
MUL	Mercaptoundecanol
MW	Molecular weight
ODT	Octadecanethiol
PBS	Phosphate buffered saline

PDMS	Poly(dimethyl) siloxane
PEG	Poly(ethylene) glycol
PS	Polystyrene
SAMs	Self-assembled monolayers
SDS	Sodium dodecyl sulfate
SPR	Surface plasmon resonance

CHAPTER 1

INTRODUCTION

Surface Interactions

The interactions between states of matter have been of intense interest to scientists for several years. It is believed that surfaces serve as communication link between atoms, ions and molecules. In addition, there are numerous applications inherent in surface interactions [1].

There are several possible outcomes when an atom or a molecule interacts with a surface. First, the atom or the molecule bounces back and in this process no energy exchange occurs between the surface and the impinging species. A second possibility is that the impinging species (atom or molecule) loses or gains energy as it rebounces from the surface. Both of these outcomes have their own advantages, but the retention of the molecule or atom on the surface is of far greater importance to the study of surface chemistry [2]. Retention of an atom or a molecule leads to two types of interactions: physisorption and chemisorption. Chemisorption results in the formation of one or more chemical bonds between the adsorbed molecule and the surface. Surface interactions have been probed extensively in research areas such as biosensor design, protein adsorption, chromatographic separations and self-assembly of monolayers [3, 4]. My thesis work is focussed on protein interactions at modified gold substrates. Hence, the

rest of this introductory chapter will be devoted to discussion on self-assembled monolayers and protein adsorption.

Protein Adsorption at Interfaces

A. Protein Structure. The fundamental units of proteins are amino acids. Amino acids in proteins are linked together by amide bonds. The sequence of amino acids in a protein describes the primary structure. There are twenty amino acids that are commonly found in proteins. The amino acids are distinguished by their side chains. It is this diversity of monomers that allow proteins to have a great variety of primary structures. Interactions between amino acids to form such structural motifs as α-helices and β-sheets govern the secondary structure. Folding of the α-helices and β-sheets generate the tertiary protein structure. The driving force behind the formation of the tertiary structure are mainly non-covalent interactions such as hydrogen bonding, ionic attractions and van der Waals interactions. The interior region of the protein molecule is usually hydrophobic whereas the hydrophilic charged groups mainly occupied the surface. The hydrophobic and hydrophilic regions also tend to fold together to keep the protein structure intact. The basic unit of the folded protein structure is the domain. The domains are the independent folded regions within the bulk structure of the protein molecule. Quaternary structure of the protein arises when multiple polypeptide chains interact to form a multidomain, complex protein molecule.

Under physiological conditions, proteins assume a single stable shape known as the native conformation. The native conformational states of proteins may usually be disrupted by adding surfactants, increasing or decreasing temperature, varying pH, applying high pressures, cleaving the disulfide bonds. These processes denature the protein, lead to loss of biological activity of the protein, and expose the interior hydrophobic groups to the exterior. Adsorption to a surface can also disrupt the native conformation of a protein. However, the extent of conformational changes depends on the flexibility of the protein.

B. Protein Adsorption. Adsorption of proteins at interfaces has received a considerable interest in recent years because of its importance in biological, medical, environmental and industrial applications. Exposure of a protein solution to an interface leads in almost all cases to adsorption of protein onto that interface [3]. The adsorption process involves a number of stages, which begin with the transportation of the protein from the bulk solution to the surface where it interacts with the surface. The interaction leads to attachment and relaxation to optimize the interaction with the surface. The relaxation process usually results in some degree of spreading of the protein molecule, involving structural rearrangements and conformational changes in the protein. Depending on the extent of relaxation, the protein molecule may detach from the surface through an exchange mechanism [5, 6]. This relaxation occurs to a greater degree on hydrophobic surfaces more than hydrophilic. Protein adsorption has been found in most cases to be irreversible

under physiological conditions. However, desorption of the adsorbed proteins can be induced by the addition of surfactant or variation in pH.

The complex structure and charge distribution of proteins enables them to adsorb to a variety of surfaces due to a combination of acting forces. The driving forces behind protein adsorption to a surface have been identified as hydrogen bonding, dipole-dipole interactions, hydrophobic interactions, ionic attractions, or entropic factors related to surface-induced conformational changes in the protein structure [7]. Protein adsorption is widely studied by a variety of techniques, yet little is known about the state of the protein after adsorption. Figure 1.01 shows that protein may adsorb onto a surface in its preferred orientation or with a change in conformation. However, the orientation and/or conformation of the adsorbed protein is influenced by the surface composition. In this thesis, the "state" of an adsorbed protein is characterized by its conformation and/or orientation. In attempt to fill this gap, much attention is now turning towards probing the conformation or the orientation of adsorbed proteins. This drive is geared towards answering questions such as: *to what extent does the adsorbed protein is denatured as a result of its interaction with the substrate material?* and *how does it relate to surface-induced conformational changes upon adsorption?* [5]. The experimental work presented in the Chapters II and III seek to address these questions using both spectroscopic and imaging techniques.

Many techniques including infrared spectroscopy (IR) [8, 9], radiolabelling, atomic force microscopy (AFM) [10, 11], surface plasmon resonance [12], circular

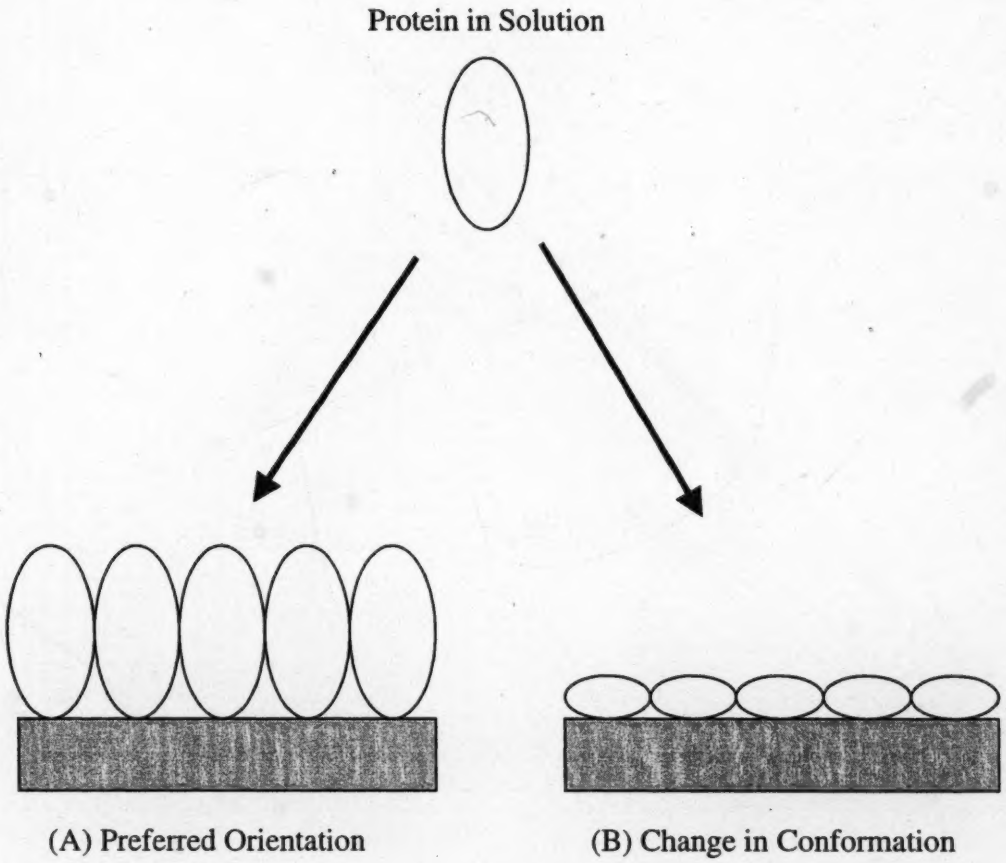

Figure 1.01. A representation showing the state of an adsorbed protein on a surface. (A) Adsorption in a preferred orientation and (B) indicates adsorption with a change in conformation.

dichroism (CD) [13], ellipsometry [13] have all been utilized to investigate protein adsorption on surfaces. All these techniques are powerful and provide valuable information on the adsorption characteristics of proteins, yet they have their own limitations. For example, the surface coverage of proteins can be determined by radioactivity measurements. Typically, the protein is radiolabelled with iodine-125 (^{125}I). After adsorption, the amount of radioactive decay is correlated with quantity of protein adsorbed. While this is a useful technique for the determination of surface coverage, no direct information about the adsorbed state is obtained. Also, the labelling process requires non-trivial synthetic steps.

Ellipsometry is also a surface-sensitive technique that provides information on the thickness, refractive index, amount and structure of the adsorbed protein. This involves measurement of a set of ellipsometric parameters, ψ and Δ, for the adsorbed protein. From ψ and Δ values, the mean refractive index and the average thickness of the protein are calculated. The values of refractive index and thickness are then employed to estimate the amount and structure of the protein based on some uncertain assumptions. However, detailed information about the structure of the protein cannot generally be obtained with this technique. This is because of the complex mathematical relationship between the ellipsometric parameters, ψ and Δ, and the molecular parameters used for describing the various substructures (α-helices and β-sheets).

AFM has become a popular technique to observe the dynamic events in the adsorption processes of proteins at the molecular level. In AFM, a sharp tip

mounted on a cantilever scans a substrate surface in a raster pattern. A laser beam reflected off the back of the cantilever and directed onto a position sensitive photodiode detector is used to monitor cantilever deflections. Maintaining a constant force between sample and tip of cantilever generates a topographic map of the surface. Surface topography provides information about the surface chemistry of the protein, which correlates to conformational changes and coverage of the adsorbed protein. However, even with the advances in AFM, tip contamination, damage of samples and imaging of weakly adsorbed molecules in liquid environment have been fundamental problems. Also, measuring the rate of protein folding has remained elusive.

IR has been used to probe conformational response of amide groups to changes in their environment to reflect possible changes in the whole protein structure. The ability to provide distinct spectral signatures for proteins (amide bands) coupled with information on coverage and conformation response make infrared spectroscopy suitable for the work presented in this thesis. Application of SPR imaging technique also offers information of adsorption characteristics of proteins in their native environment and on optical changes at the interface.

The nature of the solid surface, especially its hydrophobicity and charge density, has a strong effect on the structure and conformation of the adsorbed protein [3]. For example, hydrophobic surfaces have been observed to induce the exposure of the hydrophobic fragments within the protein molecules [3]. Even at the hydrophilic surfaces where the interaction is largely electrostatic, the

adsorption may be irreversible due to the accumulated number of protein-surface contacts may be too large to permit desorption from the surface. Thus, surface chemistry significantly influences the conformational state of adsorbed protein. Self-assembled monolayers (SAMs) of alkanethiols on gold have been used to develop molecularly well-defined surfaces for systematic studies on the influence of surface chemistry and hydrophobicity on protein adsorption.

C. Plasma Proteins. Plasma proteins utilized extensively in this work include fibrinogen, fibronectin, albimin, and lysozyme. These proteins are usually interfacially active, and their adsorption behavior is complicated by the range of different conformations their molecules can adopt when localized at the interface [3, 14]. Table 1.1 shows the molecular weight, isoelectric point and charge at physiological pH of the plasma proteins discussed below.

Fibrinogen (HFG) plays a central role in blood clotting and it is often used as a model for 'sticky' serum proteins. HFG is a 340 kD dimeric molecule consisting of two sets of three intertwined polypeptide chains (Aα, Bβ, and γ) held together by 29 disulfide bonds, three of which connect the N-termini of the dimmer subunits in an antiparallel arrangement [10, 15]. The molecule contains four major domains (two outer D domains, a central E domain and αC domain), with each having different chemical properties and degree of hydrophobicity. The overall charge of fibrinogen under physiological condition is –10 [15]. Its large size coupled with multiple charge and hydrophobic amino acid groups makes the fibrinogen molecule very surface active.

Protein	Molecular Weight (kD)	Isoelectric Point pI	Charge at pH 7.4
Human Fibrinogen	340	4.5-5.0	-10
Human Fibronectin	550	5.5-6.2	Negative*
Bovine Serum Albumin	66	4.7	-18
Lysozyme	14	11.0	+7.5

Table 1.1. Summary of the molecular weight, isoelectric point and charge at physiological pH of proteins of interest. (*) The actual value is not given in the literature.

Fibronectin (HFN) is a multifunctional extracellular matrix and plasma protein that plays a central role in cell adhesion due to its multiple binding affinities for various macromolecules found within cells, on cell surfaces and in extracellular matrices [16]. Due to the involvement of HFN with cell adhesion and other membrane interactions, its properties at interfaces are of particular interest. The HFN molecule is composed of two polypeptide chains that associate through two disulfide bonds near the COOH-terminus to form a dimmer with a molecular weight of 550 kD. The isoelectric point of fibronectin is reported between 5.5 and 6.2, and its maximum solubility occurs at pH 7.0 [17].

Bovine serum albumin (BSA) has been a long-standing acquaintance of the protein chemist, who often uses this readily available protein to block uncoated surface sites and to reduce non-specific protein adsorption to modified surfaces. BSA is a globular monomeric protein with molecular weight of about 66 kD with 35 cysteinyl residues, of which 34 residues participate in 17 disulfide bridges [18]. It has three domains and undergoes reversible conformation as a function of pH. BSA has an overall charge of –18 at neutral pH [18]. Its ability to bind to a wide variety of biological materials and surfaces results from its hydrophobic interactions and flexibility within its structure.

Lysozyme (LYS) has been studied extensively because of its robust globular structure. LYS is a small protein (14 kD) that is positively charged under physiological pH 7.4. It is composed of 129 amino acids including 18 cationic and 12 anionic residues. Its maximum surface adsorption has been shown to occur near

pH 11.0, the isoelectric point of this protein [19]. X-ray studies have revealed lysozyme as a hard, and rigid protein [19]. The stability of LYS has been attributed to the four disulfide bonds, hydrogen bonds and hydrophobic interactions among its amino acid residues. FTIR studies have also revealed that conformational changes occur upon adsorption to solid substrates [20]. LYS is often used in model studies of electrostatic adsorption of protein to surfaces.

Self-Assembled Monolayers

Investigations of organized organic monolayer films on solid substrates at the molecular scale are usually based on two methods of preparation: Langmuir-Blodgett (LB) and self-assembly techniques [2, 21, 22]. The LB technique involves the transfer of a film from air-water interface to a solid substrate whereas self-assembly is based on the spontaneous adsorption of the film components from solution directly onto the substrate. Self-assembly is much more versatile, forms stable monolayers and does not need special instrumental requirements for the assembling process. In contrast, LB films are less stable, they are maintained by weak van der Waals interactions and deposition of LB monolayers onto noble metal is often problematic [23].

The recent explosion of interest in self-assembled monolayers has been fuelled by their ease of preparation, robustness and numerous applications. The unprecedented growth in this field has its modest beginning from the earlier work by Sagiv [24]. He first described the covalent binding of octadecyl trichlorosilane

onto spin cast poly(vinyl alcohol) and later reported on synthesizing corresponding multilayers based on his previous successful results. Allara and Nuzzo have also been recognized as pioneers of recent discoveries in self-assembled monolayers by their work on spontaneous adsorption of disulfides on gold substrates from dilute solutions [25]. Deviation from the traditional moisture-sensitive alkyl trichlorosilanes used in Sagiv's work to thiols, and the use of crystalline gold surfaces were the important reasons for their success. Several other groups have also characterized these monolayers, demonstrated the use of SAMs and extended the technique to adsorption of proteins [26-32]. Alkanethiol monolayers on gold are the most studied SAMs.

To effectively determine chemical functionalities and/or composition responsible for influencing protein adsorption and conformational changes, a set of surfaces exhibiting systematic variations in surface chemistry that are stable in biological media is required. Molecular self-assembly techniques provide an effective means of fabricating organic surfaces with well-defined structure and chemistry. Therefore, in this thesis self-assembled monolayers obtained from the adsorption of different terminating functional groups of alkanethiols of the form $HS(CH_2)_nY$ where $11 \leq n \leq 18$ and $Y = CH_3$, CH_2OH and COOH on gold substrates were used. SAMs of alkanethiols on gold are stable in a variety of organic and aqueous media, making them particularly suitable for the work presented in this thesis. Gold has been widely used for monolayer studies because its reasonably inertness to oxides, strong specific reaction with sulfur even in the

presence of other functional groups. It also allows the formation of densely packed crystalline monolayers [28, 32-34].

Sulfur compounds have been shown to have a strong affinity towards coinage metal surfaces due to their ability to form multiple bonds with surface metal clusters [33]. Whitesides and co-workers have conducted kinetic studies of alkanethiols on Au(111) surface [28]. They reported that the adsorption of the alkanethiols occurs in two distinct adsorption steps. The first step is a diffusion-controlled Langmuir adsorption, which depends on the alkanethiol concentration. The second step is a surface crystallization process where the alkyl chains form two-dimensional crystal. The surface-head group interaction governs the kinetics of the first step. The second step is related to chain disorder, the different components of the chain-chain interaction and the surface mobility of chains.

The formation of SAMs representing alkanethiols on gold involves the chemisorption of the sulfur atoms of the molecule to gold surface and van der Waals interactions between the alkyl chains (CH_2 groups). Bond strength of the gold-alkylthiolate (Au-SR) bond is approximately 40 kcal/mol [23, 32]. Figure 1.02 is the schematic representation of the resulting SAM. The structure of the SAMs of alkanethiols on Au(111) has been studied using various techniques. Helium diffraction and scanning tunnelling microscopy studies reveal that the alkanethiol monolayers on Au(111) form a hexagonal ($\sqrt{3} \times \sqrt{3}$)R30° structure in which sulfur atoms occupy the three-fold hollow sites of the Au(111) surface. Infrared spectroscopic and ellipsometric measurements also indicate that the alkyl

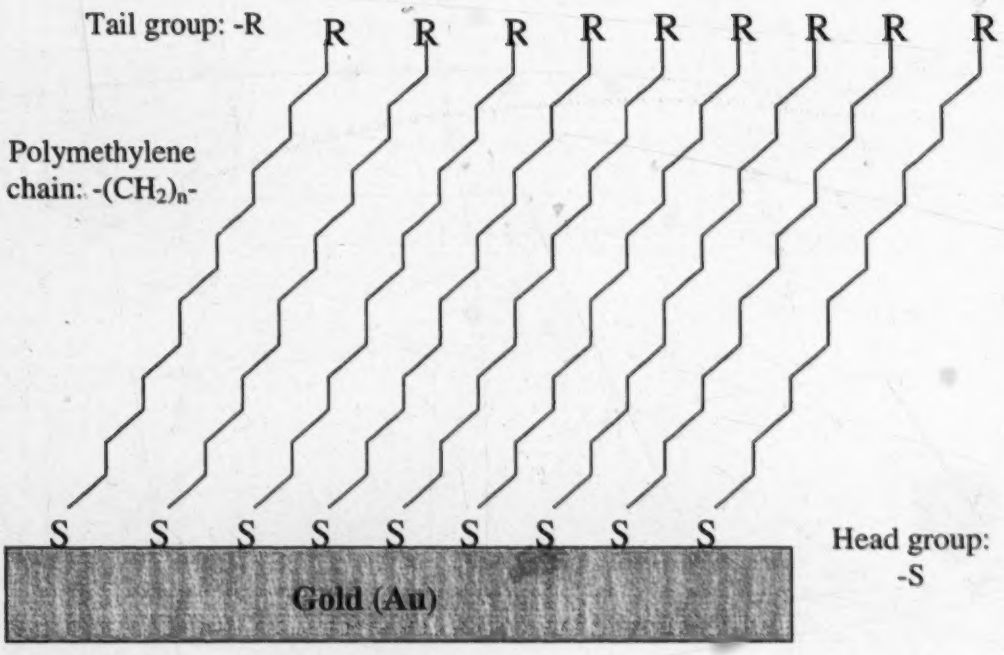

Figure 1.02. A schematic representation of the chemisorption of the alkanethiol monolayer on Au(111) substrate. The polmethylene chains are tilted by 20-30° to the surface normal. The tail group, which determines the chemistry at the solid/liquid interface, can have different functionalities such as CH_3, COOH, CH_2OH, etc.

chains are tilted from the surface normal by an angle of 20 to 30° with long-chain n-alkyl thiols displaying approximately 52 to 55° rotation about their molecular axis [26]. Sulfur-sulfur interactions are believed to be minimal with 4.99 Å spacing between adjacent sulfur atoms. The polymethylene chains have thickness in the range of 1.16 to ~1.50 Å, depending on the chain terminating functionality. Porter et al [26] have shown that long-chain thiols form well-ordered, densely packed, crystalline monolayers on Au(111), and as the chain length decreases, the structure becomes increasingly disordered with lower packing density and coverage. Moreover, the surface chemistry, structure and orientation of the terminating group of the thiol molecule determine the chemistry at the interface [27, 35]. As shown in Figure 1.02, the terminating group is the portion of the molecule that dominates the interactions that occur between the monolayer and a contacting phase. This is because the monolayers form sufficiently order and compact structures that make deeper contacts sterically forbidden.

Monolayer surfaces terminating with CH_3, CH_2OH and COOH groups have been used widely for chemical transformations [23, 36] and protein adsorption [37-40] at the solid surfaces. CH_3-terminated group of octadecanethiol presents a model well ordered, closely packed crystalline hydrophobic surface. The pKa of the hydrophilic monolayers terminating with surface-confined COOH functionality have been reported to be the range of 5-8 pK units [41]. The pH dependence of COOH group makes it useful for protein interaction studies. SAMs

of CH_2OH-terminated been used in many surface modification reactions and they are also noted for their protein adsorption resisting capabilities [38, 40, 42].

Research Objectives

The issue of conformation/orientation changes of adsorbed proteins on solid surfaces has dominated a number of biomolecular research areas due to its relevance to medicine, chromatographic separations and biosensor design among others. The role of surface chemistry in the adsorption characteristics of proteins has been widely studied using both spectroscopic and imaging techniques. The goal of my research is to use a variety of surface chemistries to probe the coverage and conformation/orientation changes of adsorbed proteins. IRRAS technique will be utilized to provide a complete picture of protein adsorption at the solid surface and SPR imaging technique for adsorption in liquid environment.

It is believed that surfaces with much higher surface energies give strong adhesive biointeractions. Hence, the initial project is to use IRRAS and Contact angle measurements to characterize the formation of thin monolayer films of alkylthiolates and polystyrene on gold substrate. The focus of this characterization scheme will be the investigation of surface hydrophobicity and compositions at the molecular scale. Probing of the quantity of adsorbed protein will form the bulk of the second aspect of my research. The state of the adsorbed protein will also be investigated. The IRRAS technique will again be employed to probe the adsorption of lysozyme (MW = 14 kD), bovine serum albumin (MW = 66 kD),

and higher molecular weight proteins of fibrinogen (MW = 340 kD) and fibronectin (MW = 550 kD).

In Chapter III, a novel SPR imaging technique will be used to provide further analysis and information on protein conformation in its native environment. Surfactant elution of adsorbed fibrinogen and fibronectin as well as antibody binding to these proteins will be discussed. SPR imaging is complementary to IRRAS studies in that IRRAS provides information on chemical structure while SPR imaging gives direct measurement of surface adsorption and optical thickness changes. The work described in the following chapters is aimed at achieving these objectives.

References

1. B. D. Ratner and S. C. Porter, in Interfacial Phenomena and Bioproducts (J. L. Brash and Wojciechowski, eds.), Marcel Dekker, Inc., New York, USA, 1996, p. 57.

2. E. M. McCash, in Surface Chemistry (M. Levitt, ed.), Oxford University Press Inc., New York, USA., 2001, p. 53.

3. J. L. Brash and T. A. Horbett, in Proteins at Interfaces II: Fundamentals and Applications (T. A. Horbett and J. L. Brash, eds.), American Chemical Society, Washington, D. C., 1995, p. 1.

4. T. A. Horbett and J. L. Brash, in Proteins at Interfaces: Physicochemical and Biochemical Studies (J. L. Brash and T. A. Horbett, eds.), American Chemical Society, Washington, DC, 1987, p. 1.

5. W. Norde and C. E. Giacomelli, Macromol. Symp. 145:125 (1999).

6. T. Vermonden, C. E. Giacomelli, and W. Norde, Langmuir 17:3734 (2001).

7. W. Norde, Macromol. Symp. 103:5 (1996).

8. B. Liedberg, B. Ivarsson, P.-O. Hegg, and I. Lundstrom, Journal of colloid and interface science 114:386 (1986).

9. B. Liedberg, B. Ivarsson, I. Lundstrom, and W. R. Salaneck, Progr. Colloid & Polymer Sci. 70:67 (1995).

10. P. Sidney Sit and R. E. Marchant, Thromb. Haemost. 82:1053 (1999).

11. T. C. Ta and M. T. McDermott, Anal. Chem. 72:2627 (2000).

12. R. J. Green, R. A. Frazier, K. M. Shakesheff, M. C. Davies, C. J. Roberts, and S. J. B. Tendler, Biomaterials 21:1823 (2000).

13. A. Ulman, in An Introduction to Ultrathin Organic Films: From Langmuir-Blogett to Self-Assembly, Academic Press, Inc., New York, USA, 1991, p. 1.

14. J. D. Andrade, V. Hlady, L. Feng, and K. Tingey, in Interfacial Phenomena and Bioproducts (J. L. Brash and P. W. Wojciechowski, eds.), Marcel Dekker, Inc., New York, USA., 1996, p. 19.

15. L. Feng and J. D. Andrade, in Proteins at Interfaces II: Fundamentals and Applications (T. A. Horbett and J. L. Brash, eds.), American Chemical Society, Washington, D. C., 1995, p. 67.

16. R. Erkki, Ann. Rev. Biochem. 57:375 (1988).

17. V. Vogel, in Proteins at Interfaces II: Fundamentals and Applications (T. A. Horbett and J. L. Brash, eds.), American Chemical Society, Washington, DC, 1995, p. 505.

18. T. J. Peters, Advances in Protein Chemistry 37:161 (1985).

19. F. Sarmiento, J. M. Ruso, G. Prieto, and V. Mosquera, Langmuir 14:5725 (1998).

20. G. Kim, M. Gurau, J. Kim, and P. S. Cremer, Langmuir 18:2807 (2002).

21. J. H. Fendler, Chem. Mater. 8:1616 (1996).

22. R. Popovitz-Biro, K. Hill, E. Shavit, D. J. Hung, M. Lahav, L. Leiserowitz, J. Sagiv, H. Hsiung, G. R. Meredith, and H. Vanherzeele, Journal of American Chemical Society 112:2498 (1990).

23. L. H. Dubois and R. G. Nuzzo, Annu. Rev. Phys. Chem. 43:437 (1992).

24. J. Sagiv, Isr. J. Chem. 18:339 (1979).

25. R. G. Nuzzo and D. L. Allara, J. Am. Chem. Soc. 105:4481 (1983).

26. M. D. Porter, T. B. Bright, D. L. Allara, and C. E. Chidsey, J. Am. Chem. Soc. 109:3559 (1987).

27. C. D. Bain, J. Evall, and G. M. Whitesides, J. Am. Chem. Soc. 111:7155 (1989).

28. C. D. Bain, E. B. Troughton, Y.-T. Tao, J. Evall, G. M. Whitesides, and R. G. Nuzzo, J. Am. Chem. Soc. 111:321 (1989).

29. C. D. Bain and G. M. Whitesides, J. Am. Chem. Soc. 111:7164 (1989).

30. C. A. Widrig, C. A. Aives, and M. D. Porter, J. Am. Chem. Soc. 113:2805 (1991).

31. M. Sprik, E. Delamarche, B. Michel, U. Rothlisberger, M. L. Klein, H. Wolf, and H. Ringdorf, Langmuir 10:4116 (1994).

32. A. Ulman, Chemical Reviews 96:1533 (1996).

33. H. Sellers, A. Ulman, Y. Shnidman, and J. E. Eilers, J. Am. Chem. Soc. 115:9389 (1993).

34. P. E. Laibinis, G. M. Whitesides, D. L. Allara, Y.-T. Tao, A. N. Parikh, and R. G. Nuzzo, J. Am. Chem. Soc. 113:7152 (1991).

35. E. Cooper and G. J. Leggett, Langmuir 15:1024 (1999).

36. J. R. Colorado, R. J. Villazana, and R. T. Lee, Langmuir 14:6337 (1998).

37. K. Prime and G. M. Whitesides, Science 252:1164 (1991).

38. G. M. Whitesides, R. E. Holmlin, X. Chen, R. G. Chapman, and S. Takayama, Langmuir 17:2841 (2001).

39. M. M. Santore and C. F. Wertz, Langmuir 18:706 (2002).

40. B. D. Ratner, C. D. Tidwell, and S. I. Ertel, Langmuir 13:3404 (1997).

41. A. Noy, D. V. Vezenov, and C. M. Lieber, Annu. Rev. Mater. Sci. 27:381 (1997).

42. M. Grunze, P. Harder, R. Dahint, G. M. Whitesides, and P. E. Laibinis, J. Phys. Chem. B 102:426 (1998).

CHAPTER II

PROBING PROTEIN ADSORPTION ON SELF-ASSEMBLED MONOLAYERS WITH INFRARED REFLECTION ABSORPTION SPECTROSCOPY

Introduction

The work presented in this chapter will demonstrate the advantages of infrared spectroscopic studies for probing changes in adsorption characteristics of protein. Protein adsorption on solid surfaces has been the focus of many scientific investigations from different disciplines [1]. This is due to its relevance to bioactivity, biocompatibility of artificial implants, cell adhesion for growth, protein chromatographic separations and fouling of contact lenses among others. Of particular interest have been investigations of the effect of surface chemistry on protein adsorption.

The biological functions of proteins depend on the correct folding of their structure, but for a protein to remain viable, it is necessary that the molecule possesses an overall stability. The complexity of protein/surface interactions is due to the fact that different proteins will interact differently and in a number of ways with different surfaces and other molecules. It is generally accepted that protein adsorption and subsequent conformational changes are greatly influenced by surface hydrophobicity [1-5]. This results in the exposure of the interior hydrophobic groups and drives attraction between neighbouring adsorbed molecules [4]. Protein adsorption studies are therefore based mainly on tracking:

(1) the amount of adsorbed protein [6, 7], (2) adsorption-desorption kinetics [4], and (3) conformational changes of adsorbed protein [3, 8]. All these investigations are geared towards understanding the behaviour of proteins in solution environment and at air/solid interface.

A number of spectroscopic and imaging techniques have been employed to elucidate the structure and/or examine changes in adsorbed protein conformation [9]. However, critical analysis of these techniques and information derived from such studies reveal that novel approaches are still required to help understand protein interfacial chemistry. For example, a sensitive technique such as fluorescence imaging, besides its requirement of fluorescent label, needs a set of protocols and quantitative analysis of acquired data is not easy [10]. Hence we took advantage of capabilities inherent in infrared spectroscopy to monitor protein adsorption on single component monolayer substrates and on bare gold surface.

One advantage of IR technique is the ease and rapidity of acquiring high quality spectra from small amounts of proteins. In addition to this, IR provides structural information of proteins in a variety of environments [3, 4, 11-14]. This makes it a useful probe for protein conformation and orientation changes. Besides, the vibrational characteristics of the peptide backbone (C=O and N-H stretches), conformational structural changes of protein molecules can be monitored by infrared spectroscopy [15]. Researchers in various disciplines have

used infrared reflection absorption spectroscopy (IRRAS) extensively for protein adsorption studies [3, 13, 16-18].

In this chapter we will use the versatile chemistry of self-assembled monolayers on gold to track the influence of interfacial chemistries on adsorbed proteins. Methyl, carboxylate and hydroxyl-terminated alkyl thiolate monolayers, as well as unmodified and polystyrene-coated gold surfaces were used for protein adsorption studies. These surfaces were chosen because of their range of chemistries. Single component monolayers were used in this study to help control surface chemistry and also to enhance interpretation and understanding of data. Contact angle measurements provided insight into surface hydrophobicity of monolayers. Adsorption of human fibrinogen, human fibronectin, bovine serum albumin and lysozyme was the main focus of this study. The diversity of the functions and interfacial chemistries of these proteins afforded us the opportunity to explore the amount of adsorbed protein and/or their conformational changes. KBr disc and IR microscope were used to obtain information on the protein crystals in their native environment. Later half of this chapter will focus on antibody binding. Information from the antigen-antibody binding was used to further explain the observed protein adsorption changes.

Experimental

Reagents and Materials. All aqueous solutions were prepared using water from a Nanopure (Barnstead, Dubuque, IA) purification system. Buffer solution

employed salts from Fisher Scientific Company. Phosphate buffered saline (PBS, pH 7.4) was prepared with reagent grade 0.2 mM KH_2PO_4 and 0.8 mM Na_2PO_4, 10 mM NaCl and 1mM KCl. Fraction I 95% clottable human fibrinogen (HFG) was obtained from Sigma (St. Louis, MO). HFG solution concentrations were 20 µg/mL in PBS. Human fibronectin (HFN) was purchased from ICN Biomedicals (Montreal, QC, Canada) and prepared to concentrations of 20 µg/mL in PBS. Goat antiserum to human fibrinogen (anti-HFG) and bovine IgG (bIgG) were purchased from ICN Biomedicals (Aurora, Ohio), diluted with PBS to achieve concentrations of 160 µg/mL. Chicken lysozyme (LYS) and bovine serum albumin (BSA) (fraction V, 99% protein) were obtained from Sigma (St. Louis, MO) and were prepared to concentrations of 100 µg/mL and 1 mg/mL respectively.

Octadecanethiol [$HS(CH_2)_{17}CH_3$] (ODT) 98%, 11-mercapto-1-undecanol [$HS(CH_2)_{11}OH$] (MUL) 97%, and 16-mercaptohexadecanoic acid [$HS(CH_2)_{15}COOH$] (MHA) 95% were purchased from Aldrich (Milwaukee, WI) and used as received except ODT which was recrystallized twice from ethanol before use. Millimolar thiol solutions were prepared in punctilious ethanol (Quantum Chemical Co., Newark, NJ). Polystyrene (PS) was purchased from Aldrich (MW = 45,000 D), dissolved in tetrachloromethane (CCl_4) and 1 mM concentrations were prepared.

Substrate Preparation. The glass substrates used were pre-cleaned in piranha solution (1:3 H_2O_2: H_2SO_4) at 90°C for 15 min, rinsed several times with

deionized water and dried with argon. Substrates for infrared reflectance absorbance spectroscopy (IRRAS) experiments were prepared by sputter coating of 300 nm of Au. A 15 nm titanium under-layer was used to ensure good adhesion of the Au film. These substrates were prepared in Microlyne (Edmonton, AB).

Monolayer Formation and Substrate Modifications. Self-assembled monolayers (SAMs) of ODT, MUL and MHA on Au for IRRAS studies were prepared from 1 mM ethanolic solutions. ODT and MUL were adsorbed overnight and MHA for 1 h. After the specified assembly time, the slides were removed from solution and rinsed well with ethanol to remove unbound thiols from the surface, and then dried with a stream of argon. Thin film of polystyrene was spin-coated onto gold slide using PWM32 Series Photoresist Spinner (Headway Research, Inc., Texas, USA).

Protein films were formed by immersing monolayer-modified Au slides in protein solution for 1 h. After the incubation period, the slides were removed from protein solution, rinsed with 1 mM PBS to remove any unbound protein and dried with a stream of argon. Antibodies were adsorbed for 2 h prior to obtaining spectra.

Infrared Spectra Measurements. IRRAS spectra were collected with a Mattson Infinity FTIR Spectrometer (Madison, WI) equipped with a low-noise mercury-cadmium-tellurium (MCT) detector cooled with liquid N_2 to about 77 K. A reflection accessory and a home-built sample holder housed in an external

auxiliary bench were employed. Spectra for modified Au slides with ODT, MUL or MHA monolayer that has been immersed in HFG, HFN, BSA, LYS and IgG protein solutions were collected. Protein adsorption on a thin film of polystyrene and bare or unmodified gold were also studied. Spectra were taken at 2 cm^{-1} resolution with a glancing angle of 86°. A self-assembled deuterated octadecanethiol, a gift from Dr. Marc Porter (Ames Lab, Iowa State), was used as the background.

Spectra of solid-phase proteins on KBr disc were acquired with a Nicolet Nic-Plan infrared microscope interfaced to a Nicolet Magna-IR 750 spectrometer. Spectra of raw protein crystal samples were also collected with this instrument.

Contact Angle Measurements. Mean advancing contact angles were measured in a laboratory atmosphere with Drop Shape Analysis System DSA 10 (Kruss GmbH, Hamburg) goniometer from Dr. Zhenghe Xu's laboratory (Univ. of Alberta, Edmonton, AB). Water from Nanopure (Barnstead, Dubuque, IA) purification system was used as thermostating liquid. Sessile drop technique was used to probe monolayer surfaces.

Results and Discussion

Characterization of Thin Films. Monolayers formed by solution self-assembly and spin-coated polystyrene films have been characterized using IRRAS and contact angle measurement techniques. The results indicated that

monolayers are crystalline and well packed, and thin films had different wettabilities.

IRRAS of thin films. To characterize the self-assembled monolayers, infrared spectroscopic measurements were made. Assignment of the bands in the C-H stretching region (high frequency region, 2700 to 3200 cm^{-1}) is of paramount importance, since the C-H region describes the chain structure of the monolayer. The peak positions for the C-H stretching modes for ODT [$HS(CH_2)_{17}CH_3$], MHA [$HS(CH_2)_{15}COOH$], and MUL [$HS(CH_2)_{11}OH$] are shown in Table 2.1. These values attest to the fact that these alkyl chains experience densely packed, crystalline-like environments [19]. The $\nu_s(CH_2)$ and $\nu_a(CH_3)$ modes are mostly selected for structural interpretation because there is minimal overlap of their absorption peaks with those of other modes. The positions of the bands are in good agreement with published data [20]. CH_2 stretching mode adsorption intensity is directly related to the number of CH_2 units per alkyl group. The infrared bands for polystyrene observed from Figure 2.01 are at 3078, 3058 and 3024 cm^{-1} which are characteristic of C-H stretching modes for monosubstituted benzene ring [21]. Bands at 2921 and 2850 cm^{-1} refer to the C-H stretching modes for the CH and CH_2 groups on the alkyl chain of the polymer. Bands in the range of 1450 to 1598 cm^{-1} are assigned to the ring C-H and alkyl C-H and CH_2 bending modes. All the characteristic bands of the monolayers are indicative of crystalline (highly-ordered) chain structures.

A

n	Monolayer	$\nu_s(CH_2)$	$\nu_a(CH_2)$
18	ODT	2850	2918
16	MHA	2851	2918
11	MUL	2850	2919

B

n	Monolayer	$\nu_s(CH_3)$	$\nu_a(CH_3)$	$\nu_s(CH_3,FR)$
18	ODT	2879	2865	2937
16	MHA	N/A	N/A	N/A
11	MUL	2879	N/A	N/A

Table 2.1. C-H stretching frequencies of ODT [$HS(CH_2)_{17}CH_3$], MHA [$HS(CH_2)_{15}COOH$], and MUL [$HS(CH_2)_{11}OH$] self-assembled monolayers on gold. n denotes the number of CH_2 units that make up the alkyl chain of the monolayer. ν_s and ν_a represent the symmetric and asymmetric stretches respectively. (A) Shows $\nu_s(CH_2)$ and $\nu_a(CH_2)$ which are respectively due to the symmetric and asymmetric C-H stretching modes of the CH_2 group of the alkyl chain. (B) Contains $\nu_s(CH_3)$ and $\nu_a(CH_3)$ which are the symmetric and asymmetric C-H stretching modes of the CH_3 group, and also $\nu_s(CH_3,FR)$ which indicates the split of CH_3 symmetric C-H stretching mode owing to Fermi resonance (FR). N/A means not applicable.

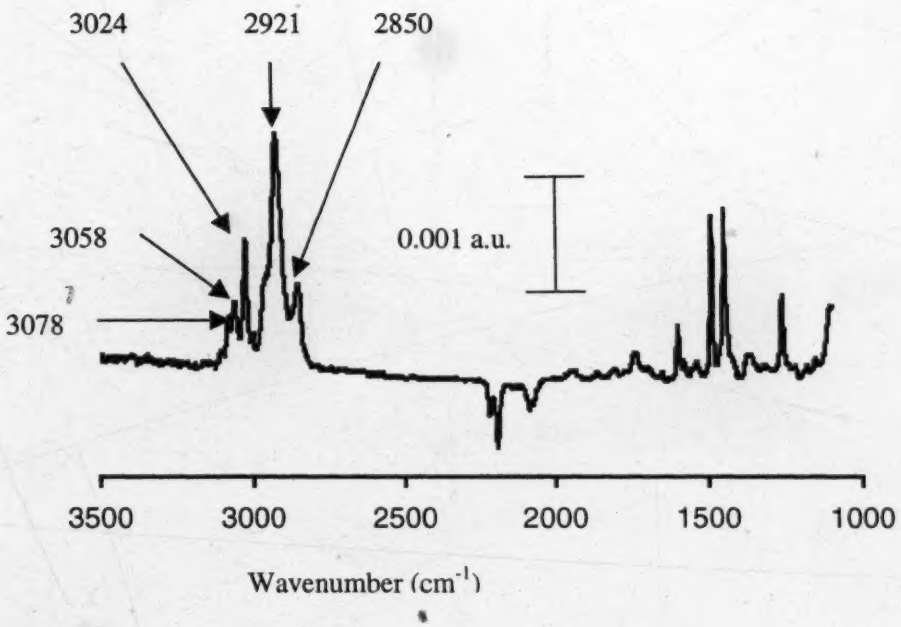

Figure 2.01. FTIR spectrum of polystyrene on gold substrate. Bands shown are characteristic of C-H stretching modes for monosubstituted benzene ring and alkyl chain of the polymer.

Contact Angle Measurement of Monolayer Films. The extent of surface hydrophobicity and wettability of monolayers and polystyrene film were determined by contact angle measurement. In order to minimize experimental errors, measurements were made on both sides of the water droplet. In addition to this, a number of readings collected at ten different spots on each surface and averaged using software. Table 2.2 summarizes the contact angle measurements of the various substrates used in this chapter. Advancing contact angle of the ODT was found to be 110 ± 1.19° while MHA gave 33.0 ± 2.20°. The θ_a for ODT is good agreement with other published results [22-26]. This confirms the greater extent of hydrophobicity of the ODT. In the case of MHA, the θ_a of 33° obtained was quite high considering the hydrophilicity of the surface COOH groups. The observed discrepancy might be attributed to adsorption of contaminants upon exposure to the laboratory atmosphere, although thorough rising with ethanol was carried out prior to analysis. However, the reported literature values for this surface ranges from 0° to about 65° [25, 27, 28]. They attributed the uncertainties in θ_a to contaminants in the distilled water used and changes in pH. MUL, however, gave θ_a = 2.0 ± 1.12° indicating far less hydrophobicity and consistent with results obtained by Whitesides and co-workers [24]. θ_a for polystyrene was 80.7 ± 1.03° consistent with results presented by other groups [3, 29, 30]. Unmodified Au showed mean advancing contact angle of 76.8 ± 3.46° that is in good agreement with the value reported by Rao and co-workers [31]. Unmodified gold is known to be relatively inert

Surface	Mean Advancing Contact Angle (θ_a)
ODT	110 ± 1.19°
MHA	33.0 ± 2.20°
MUL	2.0 ± 1.12°
Polystyrene	80.7 ± 1.03°
Unmodified Au	76.8 ± 3.46°

Table 2.2. Advancing contact angle measurements (degrees) of deionized water for ODT, MHA, MUL and polystyrene monolayer films adsorbed on gold and for unmodified gold. Values represent an average and standard deviation about that average for n = 10 measurements.

towards chemisorption of oxygen, carbon monoxide, water vapour and hydrocarbons [24]. Under atmospheric laboratory conditions, it was suspected to have physisorbed moisture and other contaminants giving rise to its relatively higher θ_a. The order of increasing hydrophobicity of the surfaces is MUL, MHA, unmodified Au, polystyrene and ODT.

IRRAS of Adsorbed Proteins. The discussion in the following section will be focussed on the effect of surface chemistry on adsorption characteristics of proteins on solid substrates. In all cases, protein concentrations were chosen to allow formation of a complete protein film after 1 h. IRRAS spectra from 2100 to 900 cm^{-1} of adsorbed proteins would be presented. In this spectral range, proteins and peptides exhibit characteristic bands, which are the direct results of vibrations in the amide linkages. The amide I band (C=O stretch) appears in the region from 1650 to 1680 cm^{-1} and the amide II band (combination of C-N stretch and N-H bend) is generally located at 1550 cm^{-1} [32, 33]. Amide I and amide II bands have been used respectively as diagnostic indicators for conformational changes and as a measure of the amount or coverage of adsorbed proteins [34, 35]. Because amide III bands in the vicinity of 1240 cm^{-1} resulting from N-H bending are weakly absorbing as compared to amide I and amide II no discussion on this band will be presented.

A. *Adsorption of Human Fibrinogen.* Fibrinogen is a massive dimeric protein (MW = 340kD) with several molecular domains. The structurally distinguishable regions of the fibrinogen molecule are: a lone central E domain,

two distal D domains, two α-helical coiled coils, two αC domains, and a pair of junctions between them [8, 36]. At pH 7.4, the E and D domains are hydrophobic and negatively charged while the αC domain is hydrophilic and positively charged. Thus fibrinogen may orient its appropriate domain to interact with different surfaces. Although, the overall charge of the molecule is –10, a negative surface may adsorb through the αC domain [8]. Fibrinogen is therefore often referred to as a "sticky" protein due its ability to adsorb onto a variety of surfaces.

Figure 2.02A shows the IRRAS spectra of HFG adsorbed on ODT (CH_3-terminated), MHA (COOH-terminated) and MUL (OH-terminated) modified Au substrates. Spectra 1 and 2 show adsorption of HFG on MUL and MHA modified Au substrates respectively. Spectrum 3 in this figure was obtained after 1 h adsorption of HFG on Au/ODT substrate. These spectra show two strong absorbances corresponding to amide I and amide II. The presence of amide peaks indicates adsorption of HFG on these three surfaces.

The spectra describing the adsorption of HFG on polystyrene modified and unmodified Au substrate are shown in Figure 2.02B. Spectrum 1 shows HFG adsorbed on polystyrene modified Au substrate whilst spectrum 2 corresponds to HFG adsorption on unmodified Au surface. This experiment was carried out to further help examine the effect of surface modifications on adsorbed protein.

Table 2.3 compares data obtained from IR spectra of HFG adsorbed on

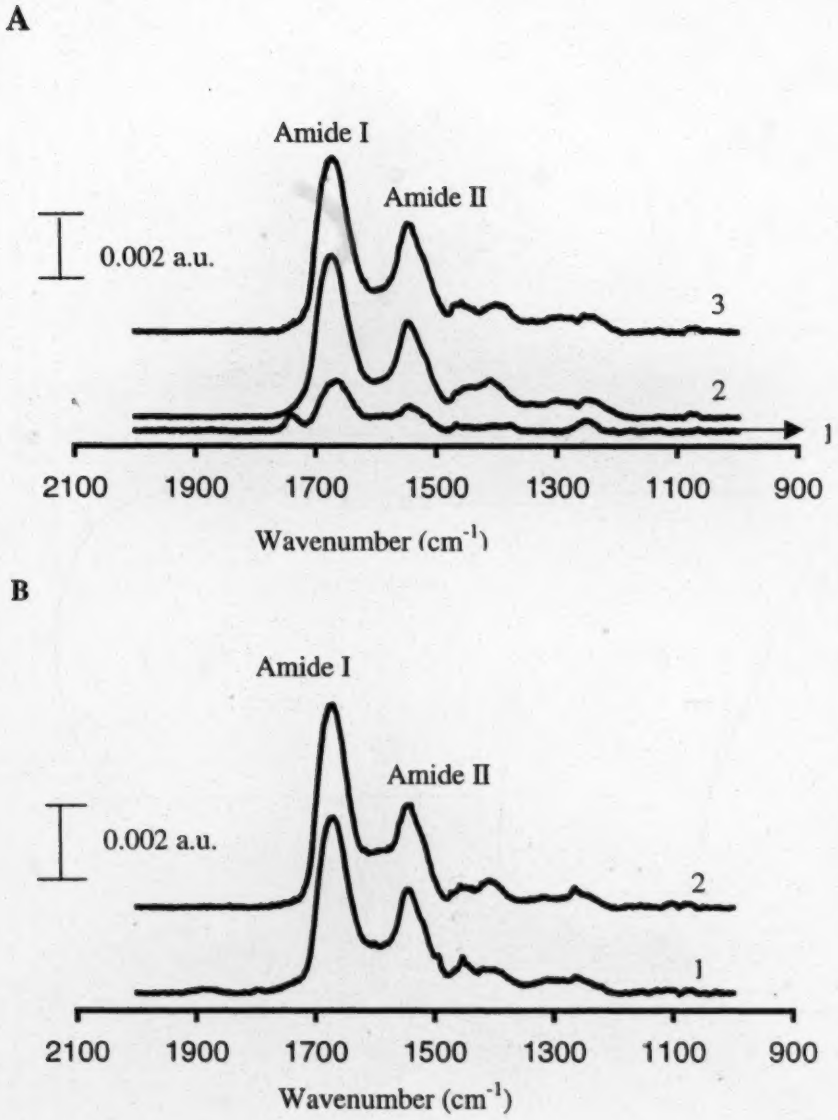

Figure 2.02. IRRAS spectra for human fibrinogen (HFG) following 1 h adsorption time on surfaces with different chemistries. (A) HFG adsorbed onto MUL (spectrum 1), MHA (spectrum 2) and ODT (spectrum 3). (B) HFG adsorption on polystyrene (spectrum 1) and unmodified Au (spectrum 2). The presence of amide peaks in each spectrum indicates that HFG did adsorbed to all these surfaces.

Substrate	Amide I ν_{aI} (cm^{-1})	Amide II ν_{aII} (cm^{-1})	Amide I Absorbance A_{aI} (a.u.)	Amide II Absorbance A_{aII} (a.u.)
ODT	1674 [a]	1545	0.0041 ± 0.0003 [b]	0.0025 ± 0.0001
MHA	1670	1546	0.0053 ± 0.0001	0.0029 ± 0.0001
MUL	1667	1547	0.0027 ± 0.0004	0.0013 ± 0.0002
Polystyrene	1670	1545	0.0043 ± 0.0001	0.0021 ± 0.0001
Unmodified Au	1674	1543	0.0058 ± 0.0001	0.0028 ± 0.0003
Solid	1650	1548	N/A	N/A
KBr	1654	1545	N/A	N/A

a: For band positions, the average value for 8 measurements is reported. In all cases, the standard deviation of the average was lower than the resolution (2 cm^{-1}) of the measurement.
b: Average value and standard deviation for 8 measurements.

Table 2.3. Spectroscopic measurements of fibrinogen (HFG) adsorbed on different surfaces and from protein crystals. Adsorbed protein spectra were collected at resolution of 2 cm^{-1} and those from solid protein and KBr at resolution of 4 cm^{-1}. N/A means not applicable.

different substrates as well as those obtained from the solid protein crystal and compressed in a KBr pellet. The positions and absorbance of the amide bands will be interpreted separately. Amide I frequency is sensitive to protein conformation [32]. In one interpretation, the amide I band is a convolution of three bands [37]. The two bands at 1687 and 1670 cm^{-1} are assigned to β-turn structures in the protein and the band at 1638 cm^{-1} represents β-sheet structures. The overall shift in the amide I band is due to variations in the relative intensities of the three primary bands due to protein conformational changes. The amide I bands of the adsorbed HFG are relatively similar. However, the samples that represent a more native protein conformation yielded significantly lower wave numbers for amide I bands than the corresponding adsorbed films (~25cm^{-1}). This suggests that the fibrinogen molecules undergo a significant degree of structural change upon adsorption onto solid surfaces. These structural changes might be the result of the intermolecular and intramolecular interactions between neighboring peptide groups and domains. A weakening of intramolecular interactions and enhanced protein-surface interaction is consistent with a distinct shift of the amide I band towards higher frequencies for adsorbed protein. Hence, protein adsorption can potentially induce conformational changes. This is consistent with similar studies carried out by Horbett and co-workers [38]. We also noted small differences in the amide I position from surface to surface (for example ODT vs MHA). Since these differences are greater than our spectral resolution, they imply surface

chemistry induced conformational variations. This is investigated further in Chapter III.

As noted previously, it has been established by other groups [1, 3, 4, 13] that proteins denature to a greater extent on hydrophobic surfaces, a process that exposes interior hydrophobic groups and drives attraction between neighboring adsorbed molecules. The peak positions of amide II bands for adsorbed HFG on the five surfaces are very similar to the solid HFG. This is not surprising since it has been shown that the amide II peak positions do not give any indication about protein conformation [3].

The absorbance of the amide II band (A_{all}) is related to the amount of protein bound to the surface. Thus, the intensities of the amide II bands serve as useful indicators for protein coverage. The similarity in amide II absorbance for ODT and MHA surfaces, as indicated in Table 2.3, implies that only a small difference in the amount of HFG is adsorbed on each functional group. In addition, the amide II peak intensities of MHA and unmodified Au are also very similar. This suggests that HFG might have similar coverage on both hydrophilic MHA surface and that of unmodified Au substrate. ODT and polystyrene surfaces showed similar peak intensities. This implies that HFG adsorbs in similar amounts on the hydrophobic ODT and polystyrene surfaces.

Figure 2.03 comparatively illustrates the amide II peak intensities and thus coverage of HFG adsorbed on each of the five substrates used in this study. HFG surface coverage on MHA is similar to that on ODT and polystyrene.

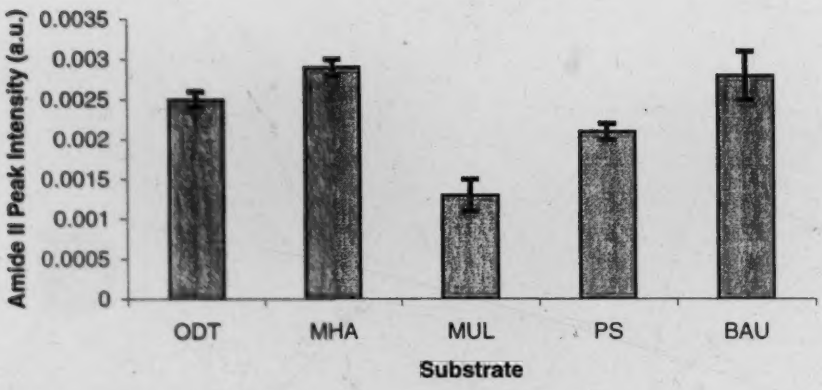

Figure 2.03. Bar graph depicting amount of HFG adsorbed on CH_3-terminated (ODT), carboxylate-terminated (MHA), hydroxyl-terminated (MUL), polystyrene (PS) and unmodified gold (BAU) surfaces.

There was less HFG adsorption on the MUL surface. This is consistent with an observation made by Santore and co-workers [39]. As noted previously [40], disruptions in interactions between MUL self-assembled monolayer and protein caused by water and PBS is suspected to be responsible for this partial HFG coverage.

B. *Adsorption of Human Fibronectin.* A brief overview of the fibronectin structural properties would be given in this section to help in the interpretation of IRRAS spectra and adsorption characteristics of fibronectin. Fibronectin is composed of two polypeptides that associate through two disulfide bonds near its COOH-terminus to form a dimer with molecular weight of about 550 kD. Each monomer strand contains a series of homologous repeating units called modules (types I, II and III modules). Clusters of several modules organize into functional domains that exhibit different binding activities. The reported isoelectric point (pI) of human fibronectin is somewhat between 5.5 and 6.2 [41].

Similar experiments and analyses to HFG were performed with HFN on ODT, MHA, MUL, polystyrene and bare Au substrates. Figure 2.04A shows the IRRAS spectra of amide region (2100 to 900 cm^{-1}) of HFN adsorbed on ODT, MHA and MUL modified Au substrates from 20 μg/mL solutions for 1 h. The presence of amide peaks is an indication of HFN adsorption. Spectrum 1 presents HFN adsorption on MUL whilst spectra 2 and 3 are show HFN on ODT and MHA surfaces respectively. The absence of amide bands in spectrum

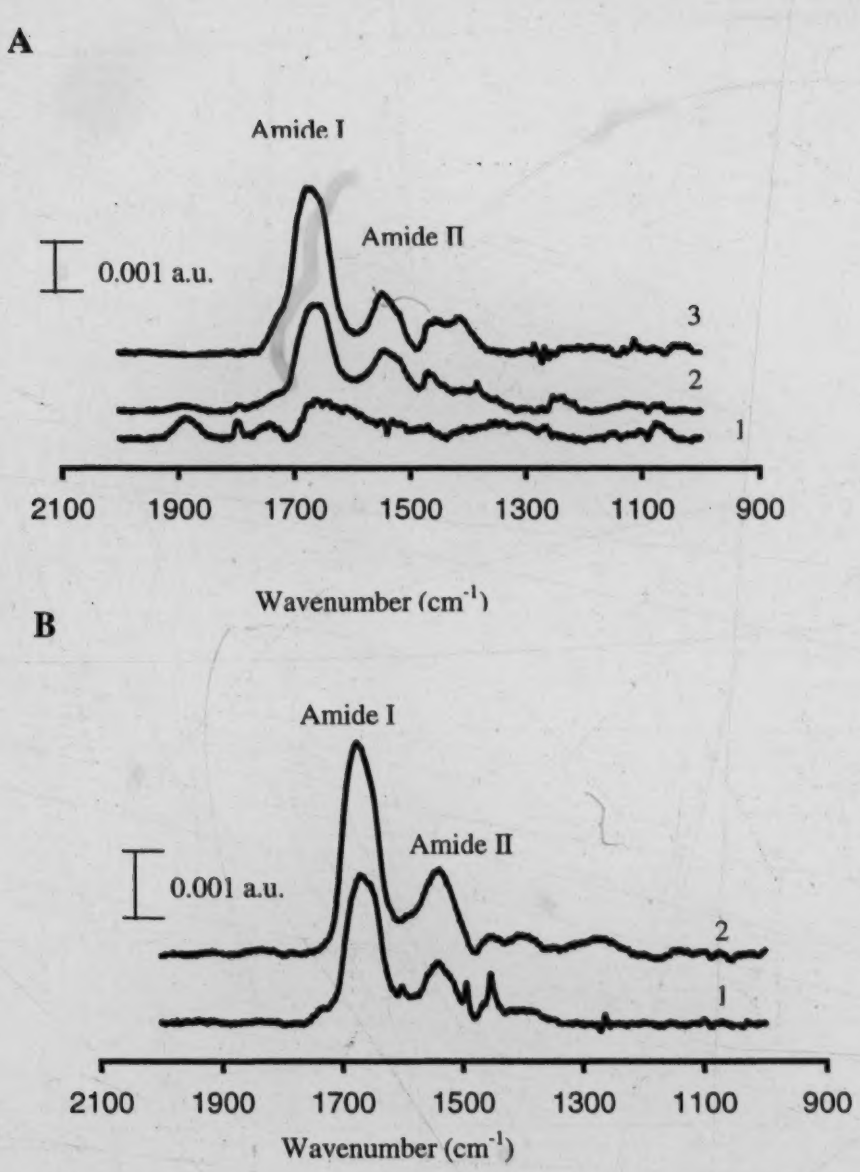

Figure 2.04. Spectra obtained by IRRAS of human fibronectin (20 μg/ml HFN) after 1 h adsorption on different surfaces. (A) HFN adsorption on MUL (spectrum 1), MHA (spectrum 2) and ODT (spectrum 3) modified Au surfaces. (B) HFN adsorbed on polystyrene-coated film (spectrum 1) and unmodified Au substrate (spectrum 2).

1 indicates that fibronectin does not adsorb significantly on the OH-terminated monolayer. The OH-terminated monolayer has been observed to have similar behavior towards proteins as "poly-ols" that are known to prevent protein adsorption [40, 42-44]. Spectrum 1 of Figure 2.04B is observed following exposure of the on polystyrene modified Au substrate to 20 μg/mL human fibronectin. Spectrum 2 corresponds to HFN adsorption on unmodified Au. Presence of typical amide bands on these substrates is a diagnostic indicator of adsorbed HFN.

Table 2.4 summarizes the IR spectroscopic data of HFN adsorption on all substrates presented in Figures 2.04A and 2.04B. It is observed from Table 2.4 that amide I bands of native HFN shifted approximately 40 cm^{-1} towards higher frequencies upon adsorption to solid surfaces. Similar to HFG, the shift in frequency of the adsorbed HFN indicates a significant change in conformation from its native structure. The amide II bands of the adsorbed protein are shifted to slightly lower frequencies compared to that of solid KBr. Although the cause of this shift is uncertain, Salaneck and co-workers [32] have attributed amide II band shift to the decreased degree of hydrogen bonding in the protein film upon adsorption to solid surface.

From Table 2.4, there are significant differences in amide II peak intensities and areas. Although HFN is known to be an adhesive protein [41, 45], it shows different adsorption behavior compared to HFG. The amide II intensities of HFN on all surfaces are significantly lower than HFG despite the

Substrate	Amide I ν_{aI} (cm^{-1})	Amide II ν_{aII} (cm^{-1})	Amide I Absorbance A_{aI} (a.u.)	Amide II Absorbance A_{aII} (a.u.)
ODT	1671[a]	1540	0.0025 ± 0.0001[b]	0.0013 ± 0.0002
MHA	1674	1546	0.0017 ± 0.0001	0.0007 ± 0.0002
MUL	-	-	-	-
Polystyrene	1669	1540	0.0018 ± 0.0002	0.0005 ± 0.0001
Unmodified Au	1667	1540	0.0028 ± 0.0002	0.0010 ± 0.0002
Solid	1632	1544	N/A	N/A
KBr	1631	1552	N/A	N/A

a: For band positions, the average value for 8 measurements is reported. In all cases, the standard deviation of the average was lower than the resolution (2 cm^{-1}) of the measurement.
b: Average value and standard deviation for 8 measurements.

Table 2.4. Tabulated spectroscopic measurements for fibronectin adsorption on the different substrates compared to its solid crystal. N/A means not applicable.

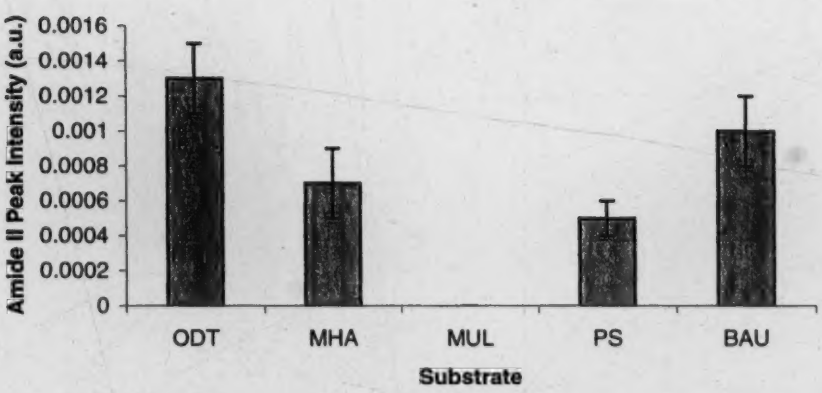

Figure 2.05. Bar graph showing the amide II band intensities of HFN on different substrates. The amide II peak intensity is used as a quantitative tool for the amount of adsorbed HFN.

fact that HFN (550 kD) is much larger than HFG (340 kD). Thus, HFG shows a greater degree of adsorption than human fibronectin consistent with other reports [46, 47]. Unlike HFG, the amount of HFN adsorbed on CH_3-terminated surface (amide II intensity = 0.0013 ± 0.0001 a.u.) is about twice that adsorbed on COOH-terminated surface (amide II intensity = 0.0007 ± 0.0001 a.u.). Grainger and co-workers carried out studies on HFN adsorption to –COOH and $–CH_3$ terminated monolayers [45]. They observed similar HFN coverage on these two surfaces after 1 h adsorption, and a significantly higher coverage on –COOH monolayer than on the $–CH_3$ surface after several hours. They attributed the variations on these two different chemistries to differences in adsorbed conformations of fibronectin on the methyl and carboxyl-terminated monolayer surfaces. However, the concentration of HFN employed in that study was ten times less than what was used in this study. The lower concentration employed might have influenced their results. It is difficult to compare our results and Grainger's work because of the differences in concentrations and methods employed for these studies. However, results obtained from both studies suggest that surface chemistry influences HFN coverage.

The graphical representation of the amount of HFN adsorbed on the different surface chemistries is shown in Figure 2.05. Based on the chemistry of the SAM surfaces, it appears that HFN has a higher affinity for hydrophobic surfaces (example ODT). Surprisingly, HFN coverage on PS is much lower than on ODT. It has been shown that HFN adsorption on PS involves unfolding

and exposure of its functional domains [48]. A significantly higher coverage of HFN was observed on unmodified Au surface but at this stage we do not have an explanation for it.

C. *Adsorption of Bovine Serum Albumin.* Adsorption of bovine serum albumin (BSA) at different surfaces used in this study showed that electrostatic attraction/repulsion forces affect the amount of adsorbed protein. Figure 2.06A shows IRRAS spectra of BSA layers adsorbed on ODT, MHA and MUL surfaces for 1 h. The IRRAS spectra for BSA adsorption on unmodified Au (spectrum 1) and polystyrene modified Au (spectrum 2) surfaces are shown in Figure 2.06B. In all cases, amide I and amide II bands are observed implying adsorption of BSA to all surfaces. Data obtained from spectral analysis are shown in Table 2.5 along with band positions from spectra of non-adsorbed BSA. As was seen with HFG and HFN, the amide I band position for adsorbed BSA is significantly blue shifted from that of solid or solution bound BSA. With the exception of MUL, which exhibited a very low coverage of BSA (see below), the amide I positions on all the surfaces agree within $\pm$ 1 cm^{-1}. This indicates that any surface chemistry conformational differences are below the detectability of the IRRAS measurement for BSA.

In Table 2.5, a close examination of amide II peak intensities of adsorbed BSA on methyl (ODT) and carboxylate (MHA)-terminated surfaces show significant differences. BSA shows greater adsorption on ODT modified surface compared to MHA. The isoelectric point for BSA is at pH 4.7 implying

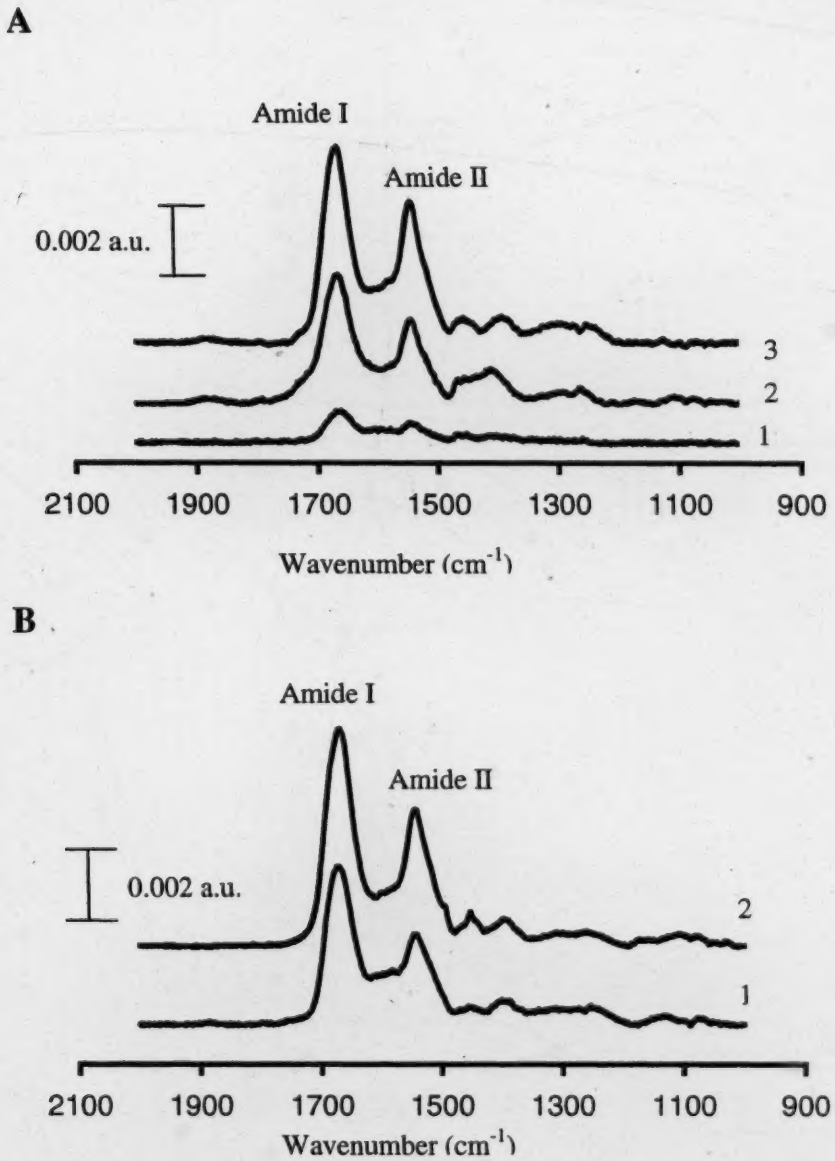

Figure 2.06. IRRAS spectra of bovine serum albumin (1mg/ml BSA) adsorbed on different substrates for 1 h. (A) Represents BSA adsorption on MUL (spectrum 1), MHA (spectrum 2) and ODT (spectrum 3) self-assembled monolayer films on Au. (B) BSA adsorbed on polystyrene modified (spectrum 1) and unmodified Au/Ti/glass substrates.

Substrate	Amide I $\nu_{aI}(cm^{-1})^b$	Amide II $\nu_{aII}(cm^{-1})^b$	Amide I Absorbance A_{aI} (a.u.)	Amide II Absorbance A_{aII} (a.u.)
ODT	1671[a]	1546	0.0049 ± 0.0003[b]	0.0034 ± 0.0001
MHA	1670	1546	0.0032 ± 0.0001	0.0020 ± 0.0002
MUL	1667	1548	0.0007 ± 0.0001	0.0003 ± 0.0001
Polystyrene	1671	1542	0.0054 ± 0.0001	0.0020 ± 0.0001
Unmodified Au	1672	1542	0.0038 ± 0.0002	0.0010 ± 0.0001
Solid	1645	1532	N/A	N/A
KBr	1655	1542	N/A	N/A

a: For band positions, the average value for 8 measurements is reported. In all cases, the standard deviation of the average was lower than the resolution (2 cm^{-1}) of the measurement.
b: Average value and standard deviation for 8 measurements.

Table 2.5. Analysis of amide I and amide II peak positions and absorbance for the adsorption of bovine serum albumin (BSA) on different substrates. Amide I and amide II peak positions of adsorbed BSA are compared with the solid BSA protein. N/A means not applicable.

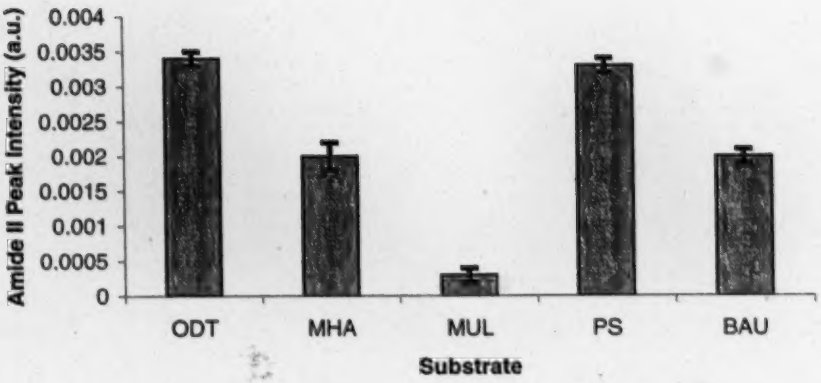

Figure 2.07. Graphical representation of the amount of BSA adsorbed on different substrates depicted by amide II peak intensity.

that the protein is negatively charged at pH 7.4 [49]. Based on the reported pKa of 5 – 8 for MHA monolayer [50, 51], the carboxylic acid groups are partially ionized to carboxylate groups upon immersion in PBS. This is supported by the presence of carboxylate peak in spectrum 2 of Figure 2.06A (1450 cm^{-1}). Hence, lower adsorption of BSA on MHA surface might be attributable to the electrostatic repulsion between the negatively charged carboxylate ions of MHA surface and the negatively charged protein. Due to the non-polar nature of the ODT surface, BSA adsorption on this surface will be mainly driven by hydrophobic interactions. The hydroxyl-terminated monolayer seems to inhibit protein adsorption as noted earlier from the discussions on HFG and HFN. From Figure 2.07, it is evident that BSA shows greater adsorption on hydrophobic surfaces than hydrophilic surfaces. This observation gives credence to the proposition that the main driving force behind BSA adsorption from solution onto solid surface is hydrophobic interactions. In addition, it has been observed elsewhere that BSA molecules exhibit large conformational adaptability [52]. As a result, it has a high affinity towards a variety of surfaces even under unfavorable electrostatic conditions [14, 49]. Hence, it is expected that surface-induced conformational changes of BSA would be mainly driven by substrate surface chemistry.

D. *Adsorption of Lysozyme.* Proteins surfaces are generally heterogeneous, having positive and negative charges as well as groups with hydrogen bonding abilities and hydrophobic regions. Hence, a small and overall

positively charged protein like lysozyme (MW ≈ 15 kD) is likely to assume different orientational and conformational states on substrates with varying surface chemistries.

Figure 2.08A shows IRRAS spectra for the adsorption of lysozyme (LYS) onto ODT, MHA and MUL modified Au substrates. LYS adsorption on MUL is presented by spectrum 1. Spectra 2 and 3 are typical IRRAS spectra of adsorbed lysozyme on methyl and carboxylate-terminated surfaces. Observance of amide bands in these three spectra proves that lysozyme indeed adsorbed on these self-assembled monolayers. Spectra 1 and 2 of Figure 2.08B indicate lysozyme adsorption on polystyrene-coated and bare Au substrates.

Table 2.6 presents the summary of infrared spectroscopic measurements of amide bands in Figures 2.08A and 2.08B. As was observed for the other proteins, there is a significant shift towards higher amide I frequencies upon LYS adsorption on solid surfaces indicating conformational change of adsorbed LYS. There are small, but measurable, differences in the amide I peak positions for lysozyme adsorbed on different surfaces. This observation indicates some surface chemistry driven differences in adsorbed conformation.

Analysis of peak intensities presented in Table 2.6 reveals that lysozyme has higher amide II intensities on MHA than ODT. This might result from electrostatic attraction/repulsion between the charged groups at the interface. Lysozyme has a net positive charge under physiological conditions [53]. Hence, the driving force behind the interaction between the adsorbed protein and

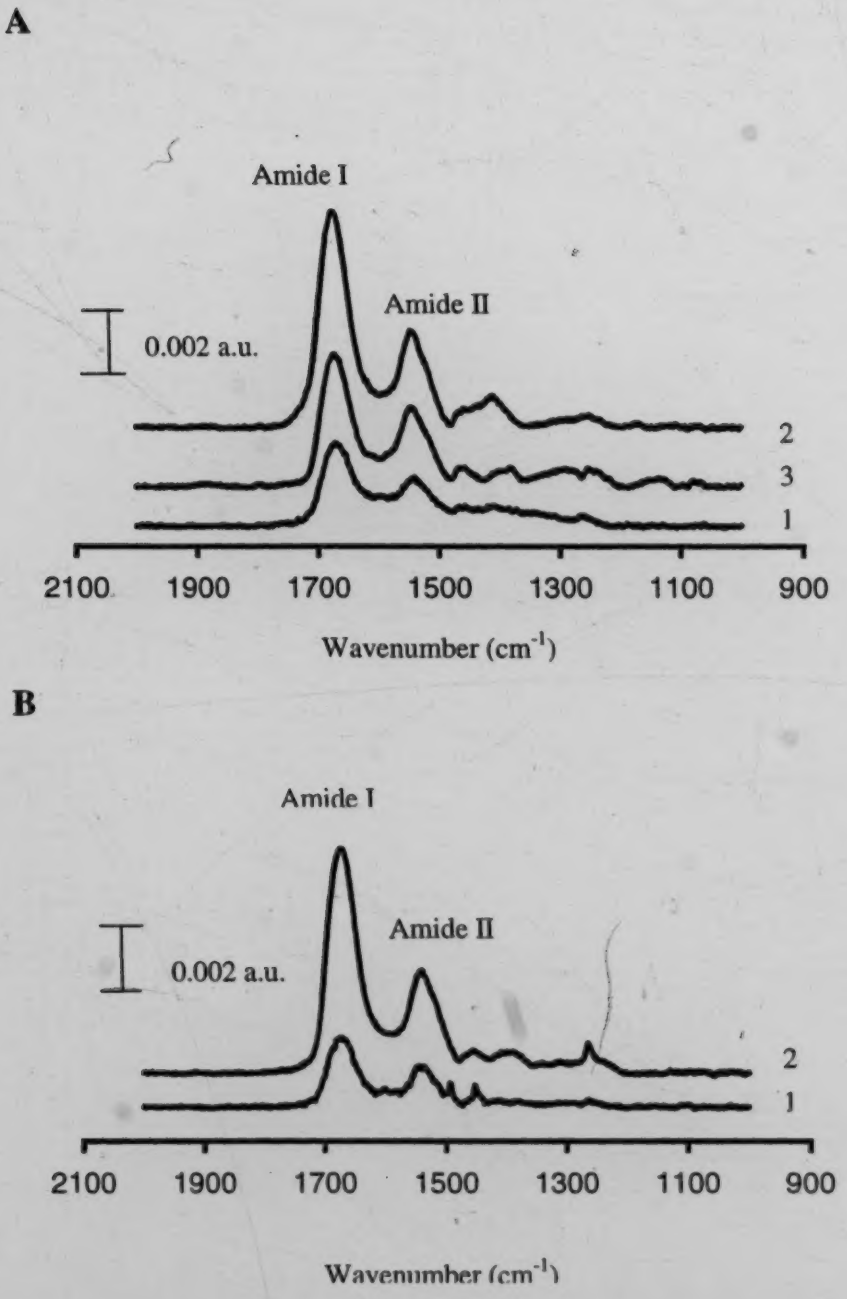

Figure 2.08. IRRAS investigation of lysozyme films (100 µg/mL LYS) adsorbed onto modified and unmodified Au/Ti/glass substrates. (A) Spectra obtained from the adsorption of LYS onto MUL (spectrum 1), ODT (spectrum 2) and MHA (spectrum 3) surfaces. (B) LYS adsorbed onto polystyrene (spectrum 1) and bare Au (spectrum 2).

Substrate	Amide I $\nu_{aI}(cm^{-1})^b$	Amide II $\nu_{aII}(cm^{-1})^b$	Amide I Absorbance A_{aI} (a.u.)	Amide II Absorbance A_{aII} (a.u.)
ODT	1671[a]	1544	0.0032 ± 0.0002[b]	0.0018 ± 0.0003
MHA	1673	1545	0.0054 ± 0.0001	0.0023 ± 0.0001
MUL	1670	1540	0.0020 ± 0.0004	0.0011 ± 0.0002
Polystyrene	1671	1540	0.0020 ± 0.0002	0.0012 ± 0.0002
Unmodified Au	1673	1540	0.0067 ± 0.0005	0.0030 ± 0.0004
Solid	1643	1536	N/A	N/A
KBr	1655	1535	N/A	N/A

a: For band positions, the average value for 8 measurements is reported. In all cases, the standard deviation of the average was lower than the resolution (2 cm^{-1}) of the measurement.
b: Average value and standard deviation for 8 measurements.

Table 2.6. Presentation of amide I and amide II band positions and intensities for adsorption of lysozyme (LYS) on different surfaces depicting different surface chemistries. N/A means not applicable.

exposed COO^- groups of MHA surface will be mainly electrostatic attraction.

Figure 2.09 shows the graphical representation of the amount of LYS adsorbed onto the various substrates employed in this study. A close examination of amide II peak intensities in Table 2.6 and Figure 2.09 show a significant amount of LYS adsorbed on ODT. This is due in part to the fact that non-polar atoms are known to occupy between 40 to 60% of the water accessible surface area of most small asymmetric proteins such as lysozyme. The incorporation of these atoms into lysozyme moiety gives it relatively high affinity to hydrophobic surfaces [54]. Again, we believe hydrophobic interactions between the denatured protein and methyl groups on ODT surface play a key role in the observed amide II peak intensity of the ODT surface. Another intriguing observation from Table 2.6 is the adsorption of lysozyme on unmodified Au. This surface showed the highest intensity for amide II. This high amide II peak intensity of lysozyme might be driven largely by electrostatic interactions and entropic factors related to surface-induced conformational changes in the protein.

In general, we observed greater LYS adsorption on hydrophilic surfaces (except MUL which is known to inhibit protein adsorption) [40] than hydrophobic surfaces. This is in agreement with earlier studies by Haynes and co-workers [55]. They observed that adsorption of LYS to surfaces result in a large shift in the average pKa of the COOH groups on the protein. This suggests that the positively charged groups on the protein surface are in close proximity

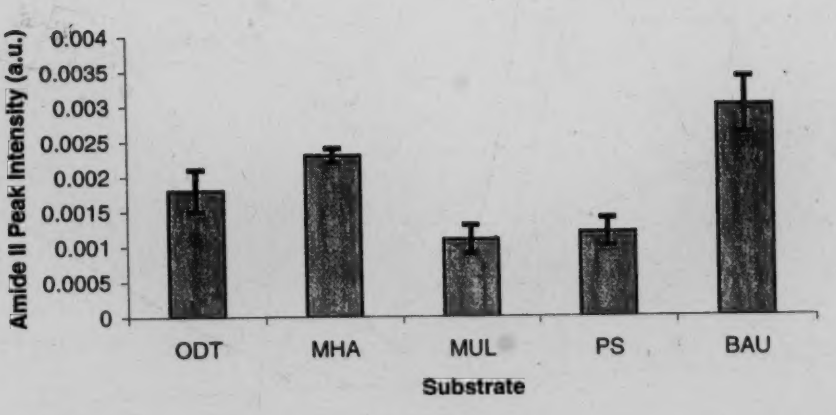

Figure 2.09. Bar graph showing the amount of lysozyme (100 μg/mL LYS) on different substrates depicted by amide II peak intensity.

to negatively charged substrates. In addition, work carried out by Penfold et al [56] supports this assertion. They demonstrated that positive charges located on the C-terminal lobe of lysozyme molecule make direct contact with the oppositely charged surfaces, and that even SDS has less effect on LYS adsorbed to surfaces due to the robust globular structure of the protein. The conclusion from the adsorption studies of lysozyme is that surface chemistry has tremendous effect on the adsorption characteristics of adsorbed lysozyme and this protein may adopt a different conformation upon adsorption to a surface. This is reflected in the observed differences in the amide I band positions observed in Table 2.6. Overall, we have found that IRRAS is a useful tool for probing the amount of adsorbed protein (amide II absorbance) and for monitoring relative differences in adsorbed conformation (amide I position).

Antibody Binding Studies by IRRAS. The aim of this study was to quantitate antigen-antibody binding after antigen adsorption onto solid surface as a further probe of changes in protein conformation. Specifically, we employed antibody binding to provide further evidence that HFG indeed adsorb in distinct conformational states on the ODT and MHA monolayers. HFG was chosen because it showed similar adsorption on ODT and MHA.

Antibodies are a group of proteins produced in response to the presence of a foreign molecule in the body. They share key structural and functional features. Functionally, they are characterized by their ability to bind to specific domains of molecules or antigens known as epitopes. There are two types of

epitopes: sequential and conformational. Sequential epitopes are defined by adjacent amino acids in the polypeptide chain whereas conformational epitopes are formed from residues adjacent in space but not necessarily in the primary sequence. If the epitopes of these antibodies are in the area of interest, then conformational dependence of antigen can be exploited as conformational changes [57]. Monoclonal antibodies have selective epitope probes. We employed polyclonal antibodies since we do not have sufficient knowledge of which epitope would be exposed after protein adsorption.

Figure 2.10A shows typical infrared reflection adsorption spectra (IRRAS) used to monitor the binding of polyclonal goat anti-HFG and bovine immunoglobulin G (bIgG) to adsorbed HFG on an ODT monolayer. bIgG was used as a control because of its similarities to anti-HFG in terms of structure. Bovine IgG is a large protein composed of two heavy chains (MW = 50 kD) and two light chains (MW = 25 kD) attached by disulfide bridges that form a Y-like structure [58].

Spectrum 1 of Figure 2.10A corresponds to HFG on ODT. Spectrum 2 results from incubation of the HFG film in 160 μg/mL bovine IgG for 2 h and spectrum 3 represents exposure of HFG film to 160 μg/mL anti-HFG for 2 h. There was a significant increase in peak intensities of all amide bands as a result of both non-specific adsorption and antibody binding to the adsorbed HFG. It was necessary to expose the HFG film to bovine IgG that adsorbs only through non-specific interaction to help address issues of physisorption of anti-HFG

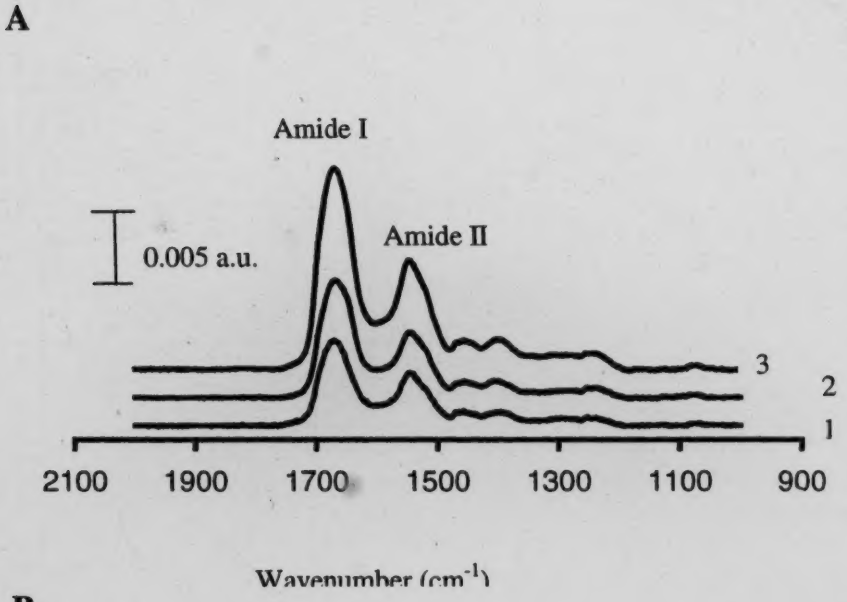

Figure 2.10. IRRAS investigation of HFG films adsorbed onto ODT and MHA modified Au surfaces, before and after exposure to anti-HFG and bovine IgG. (A) IRRAS spectra of 20 μg/mL HFG (spectrum 1), 2 h exposure of 160 μg/mL bovine IgG (spectrum 2) and 2 h exposure of 160 μg/mL anti-HFG (spectrum 3) to a surface similar to spectrum1 on ODT surface. (B) Similar experiment on MHA surface. Spectra 1, 2 and 3 are same as those of (A).

Protein	Amide II Absorbances on ODT A_{aII} (a .u.)	Amide II Absorbances on MHA A_{aII} (a .u.)
HFG	0.0025	0.0029
Anti-HFG	0.0076	0.0052
BIgG	0.0042	0.0051
Difference	0.0034	0.0001

Table 2.7. Analysis of amide II peak intensities for anti-HFG and bIgG adsorption to bound HFG on ODT and MHA modified Au substrates.

onto either the HFG film and/or the underlying substrate through surface defects. Besides this there was also the need to investigate possible displacement of HFG film by the adsorbed anti-HFG. The absorbances of the amide II bands are summarized in Table 2.7. Since the amide II absorbance tracks the amount of protein adsorbed, we can use this parameter to quantitate anti-HFG binding. Again, since bIgG can only interact with an adsorbed HFG layer through non-specific interactions, subtraction of the amide II absorbance from that of anti-HFG provides a measure of the specific antibody binding (listed as difference in Table 2.7).

Similar investigations were conducted on MHA surfaces. Figure 2.10B shows the IRRAS spectra for the adsorption on MHA surfaces while Table 2.9B gives the measurements based on the spectra. Spectrum 1 shows adsorption of HFG onto MHA surfaces in similar amounts compared to ODT surfaces ($A_{II, MHA}$ = 0.0029 ± 0.0002 a.u.). The amount of specific anti-HFG binding was computed as described above. In this case, we observed negligible anti-HFG binding to HFG on MHA. This could be due to either the conformational state of the adsorbed HFG or to the displacement of the HFG by the anti-HFG (and bIgG). In either case, the difference in antibody binding to HFG adsorbed on ODT versus MHA indicates substantial surface induced conformational differences of the HFG.

Conclusions

Our primary motivation for this investigation was the effect of different surface chemistries on protein adsorption. In this chapter, IRRAS was used to track coverage and conformational differences of proteins adsorbed onto gold substrates with different chemistries. Characterization of monolayers using IRRAS and contact angle measurements made it possible to explore the rich chemistries of all surfaces used. ODT was the most hydrophobic. OH-terminated surfaces inhibited protein adsorption due to its strong interaction with water molecules instead of protein molecules.

Application of IR microscope and KBr disc provided basis for tracking deviations from native conformation upon adsorption. All the proteins exhibited a shift in the amide bands on adsorption to solid substrates. Fibrinogen adsorbed to all the surfaces due its multidomains. Human fibronectin showed least adsorption and bovine serum albumin showed greater adsorption to hydrophobic surfaces due to its high conformational adaptability. Antibody binding to HFG further substantiated the claim of surface-induced conformation of adsorbed protein states.

The primary conclusion from this study is that we have demonstrated that IRRAS is a useful tool to study protein adsorption. In addition to this, surface chemistry plays a critical role in determining conformational state of adsorbed protein molecules. In the next chapter, patterned surfaces with distinct chemical regions will be used to further probe adsorbed protein conformation.

References

1. J. L. Brash and T. A. Horbett, in Proteins at Interfaces II: Fundamentals and Applications (T. A. Horbett and J. L. Brash, eds.), American Chemical Society, Washington, D. C., 1995, p. 1.
2. K. Prime and G. M. Whitesides, Science 252:1164 (1991).
3. D. R. Lu and K. Park, J. Colloid Interface Sci. 144:271 (1991).
4. M. M. Santore and C. F. Wertz, Langmuir 18:706 (2002).
5. G. M. Whitesides and K. L. Prime, J. Am. Chem. Soc. 115:10714 (1993).
6. J. A. Chinn, S. E. Posso, T. A. Horbett, and B. D. Ratner, J. Biomed. Mat. Res. 26:757 (1992).
7. R. J. Rapoza and T. A. Horbett, J. Biomater. Sci. 1:69 (1989).
8. L. Feng and J. D. Andrade, in Proteins at Interfaces II: Fundamentals and Applications (T. A. Horbett and J. L. Brash, eds.), American Chemical Society, Washington, D. C., 1995, p. 67.
9. B. D. Ratner and S. C. Porter, in Interfacial Phenomena and Bioproducts (J. L. Brash and P. W. Wojciechowski, eds.), Marcel Dekker, Inc., New York, USA, 1996, p. 57.
10. D. J. Graves, Trends Biotechnol. 17:127 (1999).
11. T. C. Ta and M. T. McDermott, Anal. Chem. 72:2627 (2000).
12. W. T. Surewicz, H. H. Mantsch, and D. Chapman, Biochemistry 32:389 (1993).

13. B. Liedberg, B. Ivarsson, P.-O. Hegg, and I. Lundstrom, Journal of colloid and interface science 114:386 (1986).

14. B. D. Ratner, T. J. Lenk, M. R. Gendreau, and K. K. Chittur, Journal of Biomedical Materials Research 23:549 (1989).

15. B. M. Smith and S. Franzen, Anal. Chem. 74:4076 (2002).

16. C.-Y. Ma, M. K. Rout, and W.-Y. Mock, J. Agric. Food Chem. 49:3328 (2001).

17. S. Krimm and N. G. Mirkin, J. Phys. Chem. A 106:3391 (2002).

18. P. I. Haris, G. T. Robillard, A. A. van Dijk, and D. Chapman, Biochemistry 31:6279 (1992).

19. R. G. Nuzzo, L. H. Dubois, and D. L. Allara, J. Am. Chem. Soc. 112:558 (1990).

20. M. D. Porter, T. B. Bright, D. L. Allara, and C. E. D. Chidsey, J. Am. Chem. Soc. 109:3559 (1987).

21. Z. Pei, L. Busenlehner, S. D. Worley, Y. Tang, and C. W. Curtis, J. Phys. Chem. B. 101:10450 (1997).

22. C. D. Bain and G. M. Whitesides, J. Am. Chem. Soc. 110:3665 (1988).

23. K. Abe, H. Takiguchi, and K. Tamada, Langmuir 16:2394 (2000).

24. C. D. Bain, E. B. Troughton, Y.-T. Tao, J. Evall, G. M. Whitesides, and R. G. Nuzzo, J. Am. Chem. Soc. 111:321 (1989).

25. C. D. Bain, J. Evall, and G. M. Whitesides, J. Am. Chem. Soc. 111:7155 (1989).

26. S. V. Atre, B. Liedberg, and D. L. Allara, Langmuir 11:3882 (1995).

27. J. Drelich, J. L. Wilbur, J. D. Miller, and G. M. Whitesides, Langmuir 12:1913 (1996).

28. C. D. Bain and G. M. Whitesides, J. Am. Chem. Soc. 111:7164 (1989).

29. O. N. Tretinnikov, Journal of Colloid and Interface Science 229:644 (2000).

30. J. Ji, L. Feng, Y. Qiu, X. Yu, and M. A. Barbosa, Journal of Colloid and Interface Science 224:255 (2000).

31. V. A. Tegoulia and W. Rao, Langmuir 17:9396 (2001).

32. B. Liedberg, B. Ivarsson, I. Lundstrom, and W. R. Salaneck, Progr. Colloid & Polymer Sci. 70:67 (1995).

33. R. Barbucci and A. Magnani, Biomaterials 15:955 (1994).

34. T. J. Lenk, T. A. Horbett, B. D. Ratner, and K. K. Chittur, Langmuir 7:1755 (1991).

35. B. Liedberg, B. Ivarsson, and I. Lundstrom, J. Biochem. Biophys. Met. 9:233 (1984).

36. P. Sidney Sit and R. E. Marchant, Thromb. Haemost. 82:1053 (1999).

37. S.-S. Cheng, K. K. Chittur, C. N. Sukenik, L. A. Culp, and K. Lewandowska, Journal ofColloid and Interface Science 162:135 (1994).

38. W.-B. Tsai, J. M. Grunkemeier, and T. A. Horbett, J. Biomed. Mater. Res. Part A 44:130 (1999).

39. C. F. Wertz and M. M. Santore, Langmuir 17:3006 (2001).

40. M. Sprik, E. Delamarche, B. Michel, U. Rothlisberger, M. L. Klein, H. Wolf, and H. Ringdorf, Langmuir 10:4116 (1994).

41. R. Erkki, Ann. Rev. Biochem. 57:375 (1988).

42. M. Grunze, P. Harder, R. Dahint, G. M. Whitesides, and P. E. Laibinis, J. Phys. Chem. B 102:426 (1998).

43. H. J. Kreuzer, R. L. C. Wang, and M. Grunze, J. Phys. Chem. B. 101:9767 (1997).

44. G. M. Whitesides, R. E. Holmlin, X. Chen, R. G. Chapman, and S. Takayama, Langmuir 17:2841 (2001).

45. K. B. McClary, T. Ugarova, and D. W. Grainger, J. Biomed. Mater. Res. 50:428 (2000).

46. B. D. Ratner, C. D. Tidwell, and S. I. Ertel, Langmuir 13:3404 (1997).

47. J. L. Ortega-Vinuesa, P. Tengvall, and I. Lundstrom, Journal of Colloid and Interface Science 207:228 (1998).

48. T. M. Price and M. L. Rudee, in Proteins at Interfaces: Physicochemical and Biochemical Studies (J. L. Brash and T. A. Horbett, eds.), American Chemical Society, Washington, DC., 1987, p. 48.

49. T. Vermonden, C. E. Giacomelli, and W. Norde, Langmuir 17:3734 (2001).

50. A. Noy, D. V. Vezenov, and C. M. Lieber, Annu. Rev. Mater. Sci. 27:381 (1997).

51. E. W. van der Vegte and G. Hadziioannou, J. Phys. Chem. B 101:9563 (1997).

52. T. J. Su, J. R. Lu, R. K. Thomas, Z. F. Cui, and J. Penfold, J. Phys. Chem. B 102:8100 (1998).

53. T. J. Su, J. R. Lu, R. K. Thomas, Z. F. Cui, and J. Penfold, Langmuir 14:438 (1998).

54. C. A. Haynes and W. Norde, Journal of Colloid and Interface Science 169:313 (1995).

55. C. A. Haynes, E. Sliwinsky, and W. Norde, Journal of Colloid and Interface Science 164:394 (1994).

56. R. J. Green, T. J. Su, J. R. Lu, and J. Penfold, J. Phys. Chem. B 105:1594 (2001).

57. K. L. Egodage, B. S. de Silvia, and G. S. Wilson, J. Am. Chem. Soc. 119:5295 (1997).

58. M. E. Browning-Kelley, K. Wadu-Mesthrige, V. Hari, and G. Y. Liu, Langmuir 13:343 (1997).

CHAPTER III

INVESTIGATION OF PROTEIN ADSORPTION ON PATTERNED SURFACES USING SURFACE PLASMON RESONANCE IMAGING

Introduction

In Chapter II, coverage differences in adsorbed proteins on single component substrates were investigated using IRRAS. In the IRRAS experiment, the adsorbed protein layer was removed from solution and dried prior to data collection. To follow up that work, in situ studies based on Surface Plasmon Resonance (SPR) imaging will be presented in this chapter to provide further insight into adsorption characteristics and conformational/orientation changes of proteins in their native environment. However, it is difficult to distinguish between orientation and conformation of an adsorbed protein.

Surface plasmon resonance has gained popularity in recent years for monitoring chemical changes and detecting biomolecular interactions occurring at a thin metal film surface [1-7]. The versatility of this technique stems from its numerous advantages. These include: identification of binding events with label-free molecules, high speed and sensitivity in real-time reaction monitoring, identification of specific and non-specific adsorption processes, and its in-situ and ex-situ capabilities [3].

Structurally well-defined monolayers of alkanethiols on gold have proven to be a popular vehicle for surface modification in studies on protein adsorption. Significant advances have been made in SPR over the last few years

as a biophysical sensor, enabling adsorption processes at modified surfaces to be monitored in real time [8-10]. Various researchers, notably Whitesides [11-14] and Williams [15-17], have employed SPR to monitor protein adsorption on single component monolayer surfaces. The objective of those surface modification studies is to develop a method of immobilization of proteins that would: (a) track the orientation and/or conformation changes in the adsorbed proteins [11, 14], (b) control the orientation of the immobilized protein such that the active sites would be accessible to molecules in solution [14, 18], (c) create a surface that would specifically adsorbed a protein of interest or resist non-specific protein adsorption [15], and (d) provide information about the adsorbed films and molecules on the modified surfaces [17]. However, determination of protein conformation/orientation by SPR imaging on single component monolayers is difficult and imprecise. For accurate qualitative and quantitative comparison, we employed patterned surface approach, since surface chemistry has been shown to induce changes in adsorbed protein conformation/orientation [19-21].

SPR measurements are performed in one of the following modes: (i) scanning angle SPR, in which wavelength is fixed and changes in angle and/or reflected light intensity are monitored, (ii) FT-SPR which has a fixed angle but variable wavelength, and (iii) SPR imaging [6]. In the widely employed scanning angle SPR device, the refractive index (n) is monitored in the so-called evanescent field layer, which penetrates a few hundred nanometers into

the solution from the sensor surface. Figure 3.01 is a representation of the basic optical configuration of a SPR experiment (Kretschmann geometry) consisting of a prism/thin metal film (usually Au or Ag) assembly. In this configuration, total internal reflection of light is used to excite a nonradiative surface plasmon in the metal film. A surface plasmon is a surface electromagnetic wave that propagates parallel to a metal/dielectric interface. The plasmon can be excited by light only at a well-defined angle of incidence, which occurs when the wave vector of the light in the plane of the sensor surface matches that of the surface plasmon. The resonance causes an intensity loss in the reflected light, which is seen as a sharp minimum in the reflectance. The reflected light intensity (I) is measured as a function of the angle of incidence (θ). The sharp minimum in I at the resonance angle is the experimentally recorded quantity. The surface plasmon creates an evanescent wave that decays into the solution adjacent to the metal. Thus, resonance angle strongly depends on the refractive index of the solution. Adsorption or desorption of biomolecules at the sensor surface changes the local refractive index and produces a shift in the resonance angle, which, to a good approximation, proportional to the amount of biomolecules bound to the sensor surface [6].

The SPR imaging configuration is closely related to the scanning angle SPR technique. With the imaging technique, both the angle and wavelength are fixed and change in intensity is monitored. An image of the surface is captured with a CCD camera. As shown in Figure 3.02, a collimated, polychromatic light

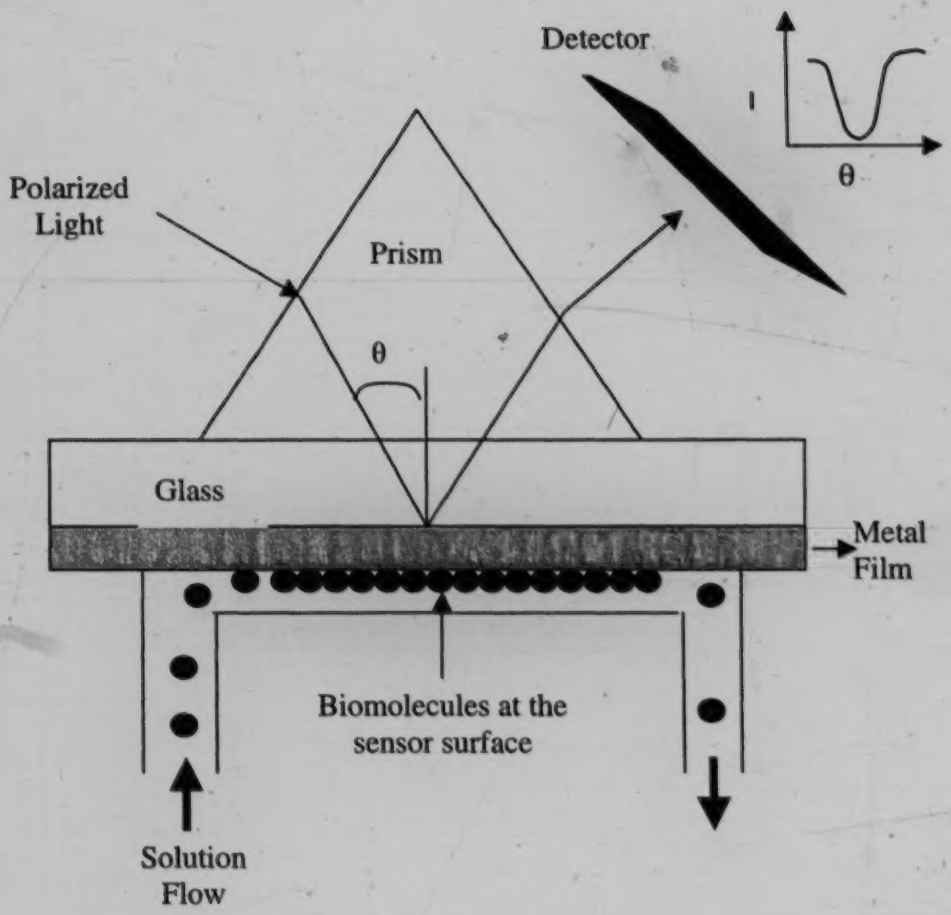

Figure 3.01. Schematic representation of the surface plasmon resonance (SPR) biosensor. At a specific angle of incidence (θ), the surface plasmon creates evanescent wave that decays into the solution at the sensor surface leading to a minimum in reflected light intensity (I).

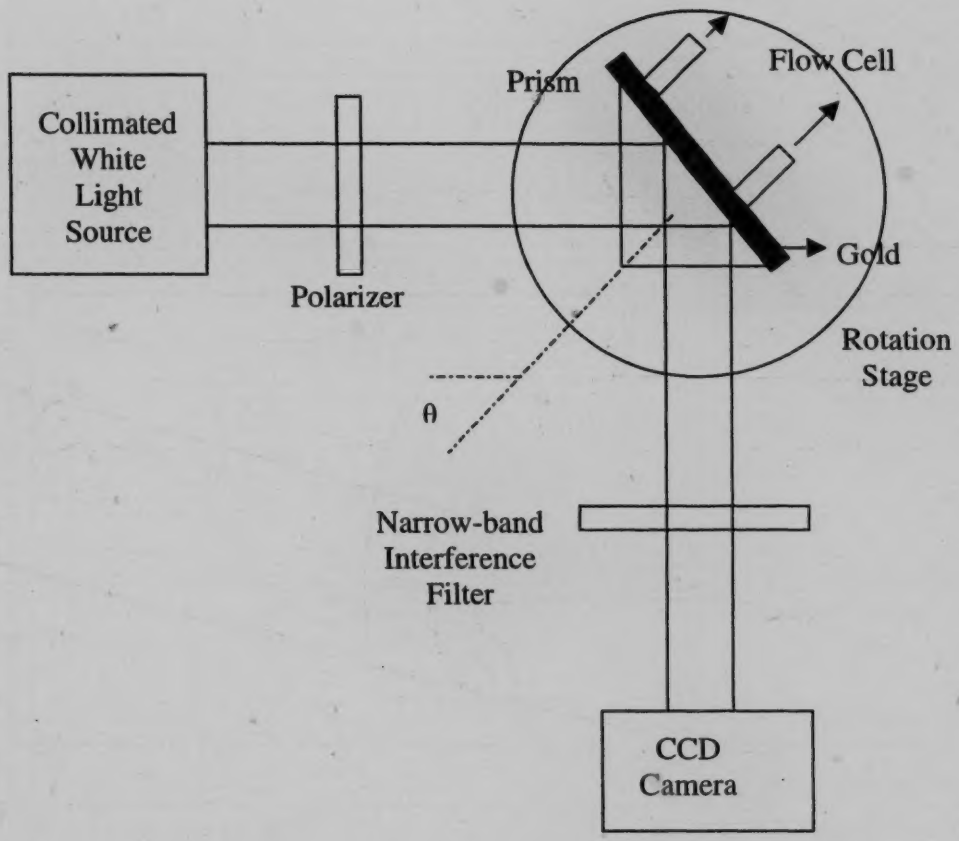

Figure 3.02. Surface plasmon resonance imaging experimental setup. Light from a collimated white light source passes through a polarizer and incidents on a prism/Au/ sample assembly at a specific incident angle, θ, near the SPR angle. The reflected light passes through a narrow-band interference filter and detected with a CCD camera.

passes through a polarizer and incident on a prism/thin gold film/sample assembly at an angle above the critical angle. The reflected light then passes through a narrow-band interference filter and is detected with a CCD camera. Real-time images are acquired as the binding reaction occurs. The prism/thin gold film/sample assembly is mounted on a rotation stage so that the incident angle can be manipulated. This allows for ease in maximizing the contrast of the patterned surface and the SPR image. The liquid flow cell attached to the assembly allows collection of in-situ images.

Human fibrinogen and human fibronectin were chosen for the SPR imaging studies because the surfaces of these proteins have been well characterized with IRRAS in Chapter II, hence we know their coverage. SDS elution and antibody binding results will be presented to further evaluate the observed conformational/orientation changes in adsorbed proteins.

Experimental

Reagents and Materials. Fraction I 95% clottable human fibrinogen (HFG) was obtained from Sigma (St. Louis, MO). HFG solution concentrations of 20 μg/mL were prepared. Human Fibronectin (HFN) was purchased from ICN Biomedicals (Montreal, QC, Canada) and prepared to concentrations of 20 μg/mL. Antiserum to human fibronectin purchased from ICN Biomedicals was prepared to concentrations of 105 μg/mL. Goat antiserum to human fibrinogen (anti-HFG) was purchased from ICN Biomedicals (Aurora, Ohio), diluted with

PBS to achieve concentrations of 160 μg/mL. All aqueous solutions were prepared using water from a Nanopure (Barnstead, Dubuque, IA) purification system. All proteins were used as received without further purification. PBS and protein solutions were filtered with a 22 μm millex-GV low-protein binding filter (Millipore, Bedford, MA) before they were used in surface plasmon resonance (SPR) imaging experiments. Buffer solution employed salts from Fisher Scientific Company. Phosphate buffered saline (PBS, pH 7.4) was prepared with reagent grade 0.2 mM KH_2PO_4 and 0.8 mM Na_2PO_4, 10 mM NaCl and 1mM KCl. Sodium dodecyl sulfate (SDS) (Electrophoresis Purity Reagent, MW=288.38) was purchased from Bio-Rad laboratories (Hercules, CA). 3% w/v SDS solution was prepared.

Octadecanethiol [$HS(CH_2)_{17}CH_3$] (ODT) 98%, 11-mercapto-1-undecanol [$HS(CH_2)_{11}OH$] (MUL) 97%, and 16-mercaptohexadecanoic acid [$HS(CH_2)_{15}COOH$] (MHA) 95% were purchased from Aldrich (Milwaukee, WI) and used as received except ODT which was recrystallized twice from ethanol before use. 2 mM thiol solutions were prepared in punctilious ethanol (Quantum Chemical Co., Newark, NJ). Poly(dimethyl)siloxane (PDMS, Slygard 184) elastomer kit was obtained from Dow Corning (Mississauga, ON).

Substrate Preparation. The high refractive index SF-10 ($n \approx 1.711$) glass (Schott Glass, 18mm x 18mm x 1mm) substrates used were pre-cleaned in piranha solution (1:3 H_2O_2: H_2SO_4) at 90°C for 15min, rinsed several times with deionized water and dried with argon. A 1 nm adhesive layer of chromium (Cr)

and 45 nm of gold were evaporated on the clean SF-10 glass substrates using a thermal evaporation system (Ion International Inc., New Windsor, NY). A vacuum of 4.6×10^{-6} mbar was used for evaporation at a rate of 0.2 Å/sec for Cr and 0.4 Å/sec for Au. Once prepared, the Au slides were rinsed using ethanol and water followed by drying with argon. The substrates were then cleaned in ozone cleaner (UVO-Cleaner, Model No. 42, Jelight Company Inc., Irvine, CA) for 10 min.

Fabrication of PDMS Stamps. Poly(dimethyl)siloxane (PDMS) stamps used for microcontact printing (μCP) were fabricated from Slygard 184 (ratio between component A and B was 1:10) according to published procedure [22]. The dimensions of the PDMS stamps were 18 mm x 18 mm x 2 mm.

Patterned Monolayer Formation. Patterned substrates used for SPR imaging were prepared by microcontact printing (μCP) using the procedure developed by Whitesides' group [22-25] followed by back-filling with a second solution. Optimal cleaning procedure for PDMS stamp proposed by Ratner *et al* [26] was used in this study. The pre-cleaned PDMS stamp was immersed in a 2 mM ODT solution for 30 min effectively inking the stamp. The stamp was then removed, rinsed with ethanol and dried under a stream of argon. Transfer of thiol molecules onto Au-coated SF-10 glass required bringing the stamp and the Au substrate into contact for a period of time, ranging from 30 to 60 s. The partially modified substrate was then immersed into 2 mM ethanolic MUL or MHA solution for 30 min. ODT was chosen for μCP because it has been shown

to exhibit greater packing density [22, 27]. The patterned substrate was then removed and rinsed with ethanol, and dried with argon prior to protein adsorption study using SPR imager. Distinct chemical regions were positioned side- by-side using μCP. Surfaces were printed with ODT and the remaining bare Au regions were back-filled via self-assembly of MHA or MUL.

Surface Plasmon Resonance (SPR) Imaging. The SPR imager was purchased from GWC Instruments, Madison, WI. The images were collected using V++ Precision Digital Imaging System Version 4.0 Software (GWC). SF-10 glass prism (n=1.711) was used to couple monochromatic light into the Au/thin film/sample assembly. Light reflected from this assembly was collected via a CCD camera to produce SPR images. An index matching fluid (n=1.72) layer was used between the prism and the back of Au/thin film/sample assembly to reduce back-reflection and to avoid fringing effects. All buffer and protein solutions were de-aerated with a stream of argon prior to solution flow to minimize bubble formation during image capture.

Results and Discussion:

The results from SPR imaging technique on the adsorption of HFG and HFN in solution to patterned CH_3 and COOH monolayers will be presented. All images presented are difference images.

HFG Adsorption on Patterned Monolayers. Figure 3.03A is an SPR image, collected in PBS, of an ODT/MHA patterned substrate. The observed

contrast indicates a variation in refractive index at each component. The variation is likely due to slight differences in the chain lengths and thus the thickness of these two monolayers (ODT ≈ 23 nm, MHA ≈ 20 nm) [28-30] and the interactions of the solvent with the vastly different chemical head-groups.

Exchanging the PBS solution with 20 μg/mL HFG in PBS and equilibrating for 1 h results in the image shown in Figure 3.03B. The change in contrast from Figure 3.03A is due to the adsorption of HFG to the ODT/MHA patterned surface. Figure 3.03C is the difference image when Figure 3.03A is subtracted from Figure 3.03B, and shows contrast that is not influenced by that of the substrate. The variation in SPR signal at each functional group, MHA (brighter region) and on ODT (darker contrast), can be attributed to differences in the amount of HFG adsorbed or differences in the adsorbed state of HFG on each functional group. If the observed contrast in Figure 3.03C is due to differences in the amount of adsorbed protein, then the direction of contrast implies a greater surface coverage of HFG on the COOH-terminated MHA monolayer relative to ODT. However, the IRRAS results presented in Chapter II suggests that HFG adsorbed to both MHA and ODT in similar amounts (Amide II absorbances of 0.0025 and 0.0029 a.u. for ODT and MHA respectively).

In order to ensure that SPR image contrast tracks IRRAS coverage measurements, we examined the adsorption of HFG on a patterned surface consisting of ODT and 11-mercapto-1-undecanol (MUL). Recall from Chapter

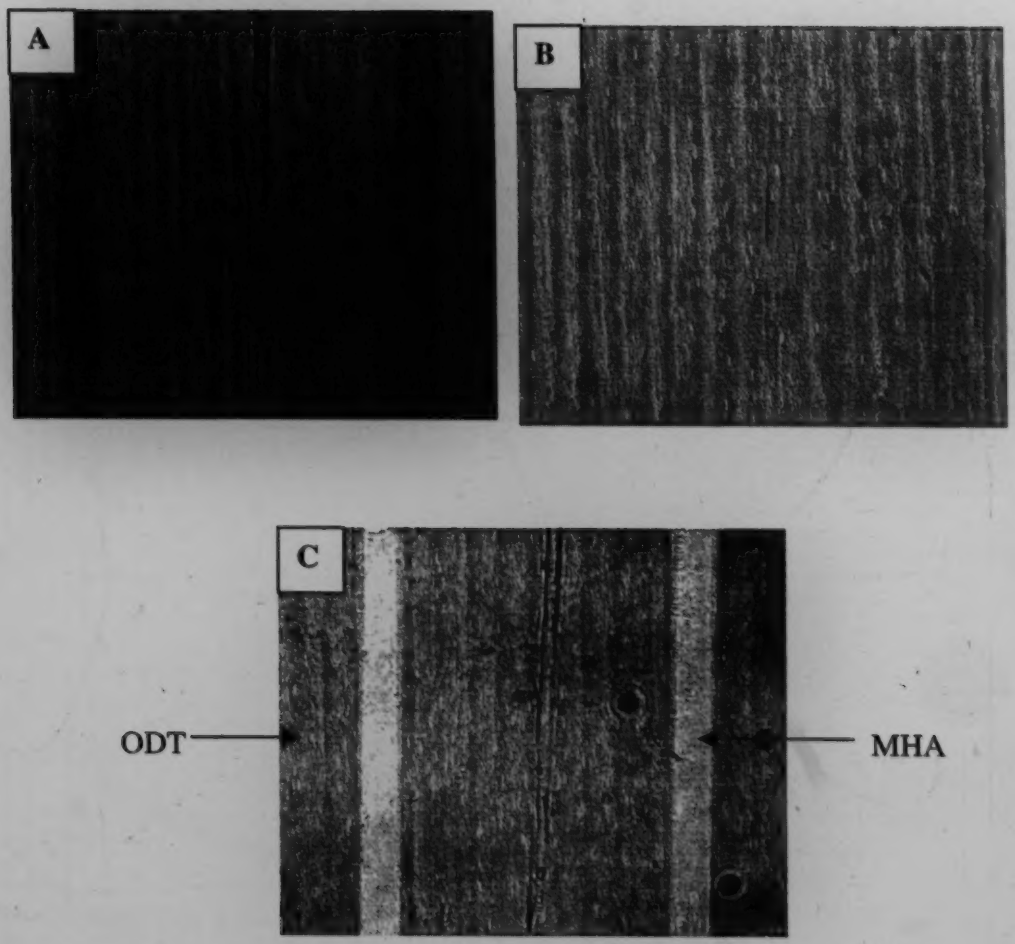

Figure 3.03. Adsorption of human fibrinogen (HFG) on ODT/MHA patterned monolayer surfaces. (A) SPR image collected in 1 mM PBS solution. (B) Raw image following adsorption of 20 μg/mL HFG on ODT/MHA patterned surface. (C) SPR difference image obtained from the subtraction of image A from image B. Brighter regions of the image show HFG on MHA surface and darker regions indicate HFG on ODT monolayer film.

Figure 3.04. Indicates SPR difference image showing HFG adsorption on ODT/MUL patterned substrate. Brighter contrast represents HFG adsorption on ODT monolayer and darker regions for HFG on MUL.

II that the surface coverage of HFG to ODT monolayer is much greater than on MUL (Amide II absorbances of HFG on ODT = 0.0025 a.u. and MUL= 0.0013 a.u.). Figure 3.04 is the difference image following adsorption of HFG to an ODT/MUL patterned surface for 1 h. The MUL region shows a darker contrast consistent with little or no HFG adsorption. A much higher signal was observed on the ODT surface as expected based on IRRAS coverage results. Thus, SPR image contrast does correspond to expected variations in surface coverage as determined by IRRAS.

Since IRRAS measurements suggest that a similar amount of HFG is adsorbed to ODT and MHA, the contrast observed in Figure 3.03C is likely due to differences in the state of adsorbed protein. The adsorbed state can be characterized by the orientation of the protein and/or by conformation. The effect of the adsorbed state on SPR contrast will be examined in the next section.

SDS Elution of HFG on ODT/MHA Patterned Substrate. Ionic surfactants, such as sodium dodecyl sulfate (SDS), are known to interact with proteins in solution [31-33]. These interactions result in the formation of surfactant-protein complexes that have different properties from those of the pure protein. In addition, the surfactant-protein complexes have been shown to result from hydrophobic interactions that are influenced by conformational/orientation changes in the adsorbed protein [33]. Hence, there

have been some attempts in recent years to characterize surface-induced changes of adsorbed proteins using surfactant elution [31, 33].

Figure 3.05A is the image captured before eluting HFG with SDS. The brighter regions correspond to HFG adsorption on MHA and darker region to HFG on ODT similar to Figure 3.03C. This surface was exposed to 3% w/v SDS solution for 30 min. The cell was rinsed with PBS and an image was collected. Figure 3.05B is the difference image obtained by subtracting the raw image after HFG adsorption from the raw image after SDS elution. Since both raw images contained the background substrate, Figure 3.05B represents only the effect of elution of protein with SDS. The darker contrast (lower signal) on MHA regions reflects a greater amount of HFG eluted relative to the ODT region.

This is the first time SPR imaging has been employed for the simultaneous detection of protein elution from different surfaces. Based on earlier conclusions of elution results [32, 34], we believe the difference in HFG elution shown in Figure 3.05B reflects a variation in adsorbed conformation/orientation of HFG on ODT relative to MHA. Furthermore, the lower elutability of HFG from the CH_3-terminated ODT surface implies that a more tenaciously bound HFG layer forms on ODT. This result indicates that the SPR contrast observed when HFG adsorbs to a patterned ODT/MHA substrate can be attributed to differences in the adsorbed conformation/orientation of the protein. To further confirm this, we used antibody binding presented below.

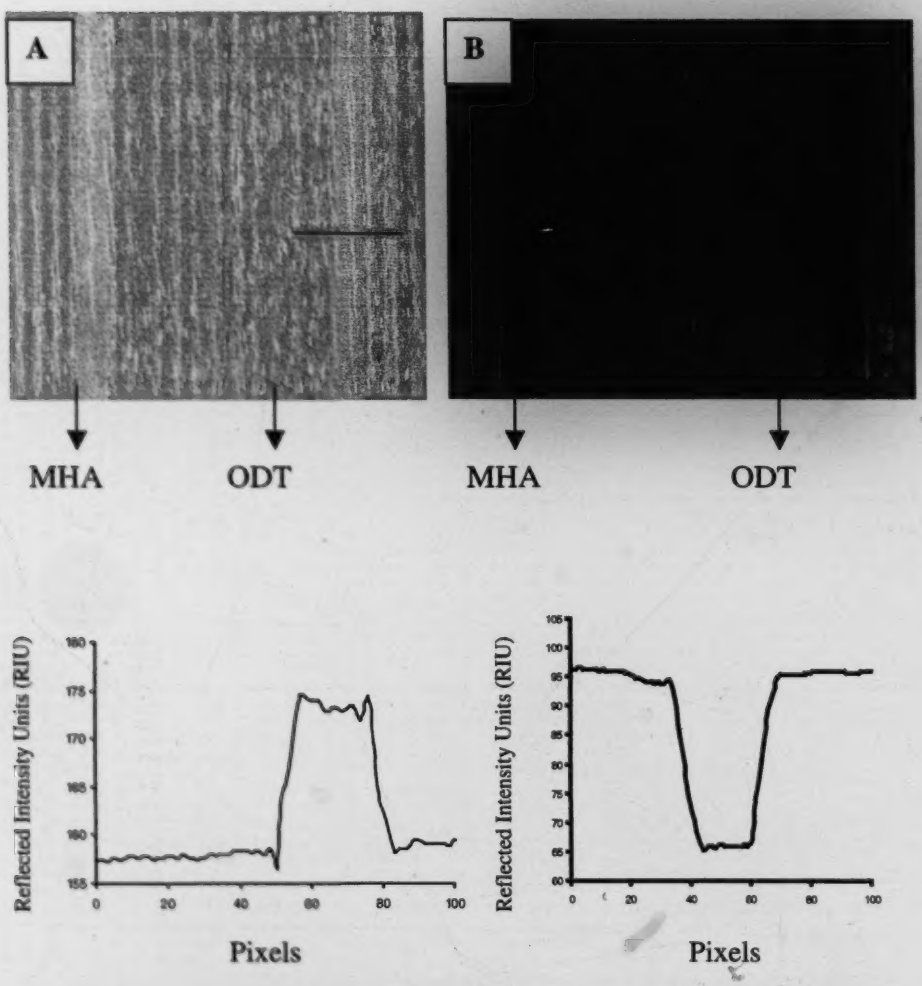

Figure 3.05. SPR difference images showing SDS elution of adsorbed HFG on patterned gold substrates. (A) Before SDS elution of HFG on ODT/MHA patterned surface. Brighter regions indicate HFG adsorbed on MHA (COOH-terminated) monolayer surface and darker regions show HFG on ODT (CH_3-terminated) monolayer. (B) SPR difference image obtained after SDS elution of HFG. The change in contrast of image as observed in (B) is an indication of the removal of HFG by SDS. The lines drawn in images A and B indicate regions where cross-section profiles were taken.

Anti-HFG Binding to HFG. It has been shown that the conformation/orientation of an adsorbed protein influences the amount of antibody binding [7, 35]. Thus, the main focus of this section is to use antigen-antibody interactions to further explore conformational/orientation changes in adsorbed fibrinogen and fibronectin. SPR imaging is an ideal technique for the detection of interactions of antibodies with their respective antigens since radioactive or fluorescent labeling which may adversely affect the antibody structure is not required. The use of patterned monolayer arrays made it possible to explore the role of surface chemistry on protein adsorption and subsequent antibody binding.

Figure 3.06A is the difference image showing the contrast after HFG adsorption from a 20 μg/mL solution. Figure 3.06B is the difference image resulting from the subtraction of the raw image after HFG adsorption from the raw image after exposure to 160 μg/mL anti-HFG and rinsing with PBS. Thus, the observed contrast is due only to differences in antibody binding at each region. From the cross-sectional profile, anti-HFG binding to the HFG/CH_3 region increases the reflected intensity by 144 RIU while antibody binding to HFG adsorbed to COOH region results in an increase of 156 RIU.

We believe that the greater antibody binding at HFG/COOH region indicates that the protein is less denatured when adsorbed to MHA layer relative to ODT surface. This is consistent with the idea that proteins must unfold significantly to interact or adsorb to hydrophobic surfaces. Importantly, the

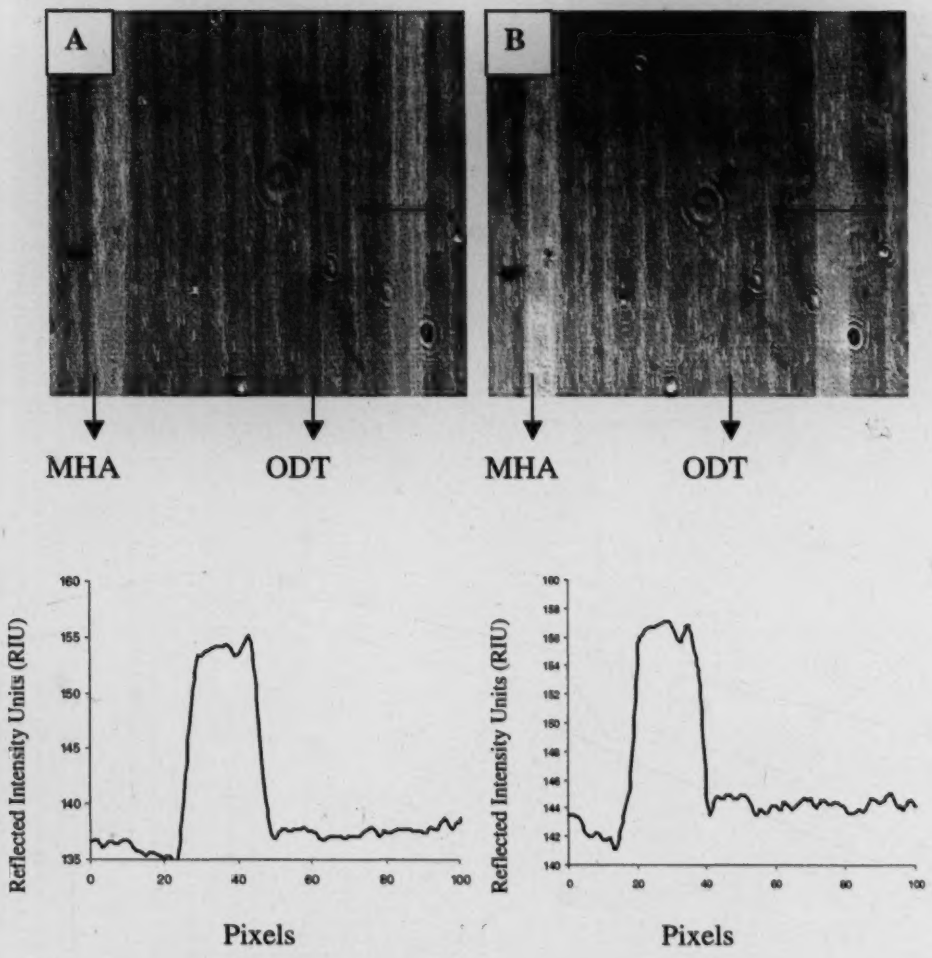

Figure 3.06. SPR difference images showing antibody binding to HFG adsorbed to patterned monolayers. (A) Difference image after the adsorption of 20 μg/mL HFG on ODT/MHA patterned surface. (B) Difference image after the exposure of adsorbed HFG to 160 μg/mL anti-HFG. The reflected intensity profiles are used as quantitative tools to indicate the amount of protein adsorbed. Lines shown in images A and B show the region cross-section profiles were taken.

antibody study provides evidence that HFG adsorbs in different conformations/orientations on COOH- and CH_3-terminated monolayers and that the contrast apparent in Figure 3.06A is due to those conformational/orientation differences. Thus, SPR imaging can map differences in protein adsorption on patterned monolayers.

HFN Adsorption on Patterned Monolayers. The adsorption of human fibronectin (HFN) to patterned alkylthiolate monolayer surface was carried out to further explore surface-induced changes in proteins. Figure 3.07A is an SPR difference image following adsorption of HFN on ODT/MHA patterned substrate for 1 h. The MHA region shows a brighter contrast correlating with a higher quantity of adsorbates on MHA region than the ODT region. The variation in SPR signal on the two different chemistries can be attributed to either differences in the amount of HFN adsorbed or differences in the adsorbed state of the protein as shown above for HFG. Recall that the IRRAS results obtained in Chapter II showed higher HFN coverage on ODT relative to MHA (Amide II absorbance for ODT = 0.0013 a.u. and MHA = 0.0007 a.u.). This indicates that HFN exhibits different adsorption behavior in solution and in its adsorbed state in air as used in the IRRAS studies. For HFN, we believe that the changes in signal intensity on the MHA and ODT regions may result from differences in surface-induced conformations/orientations of the adsorbed HFN. This conclusion is not surprising based on the fact that hydrophobic surfaces have been shown to induce dramatic denaturation of HFN, causing proteins to

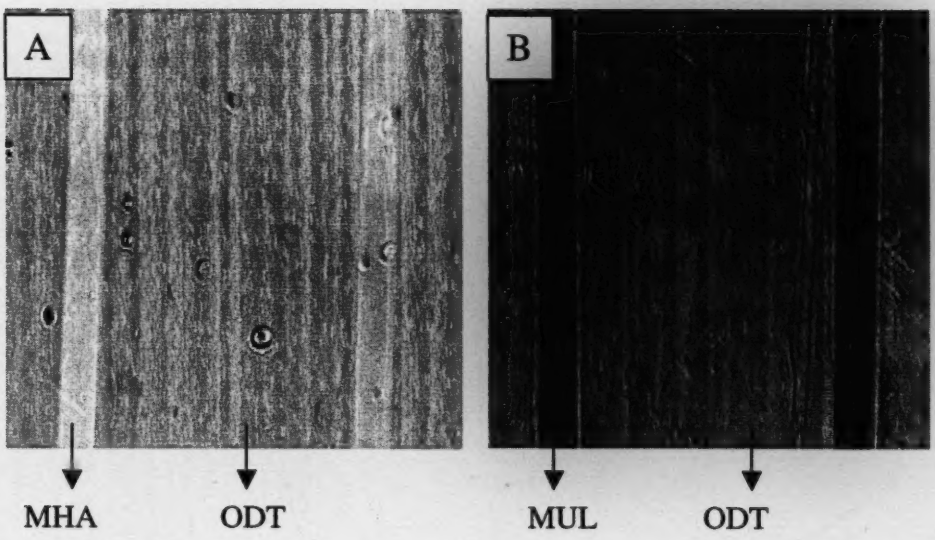

Figure 3.07. SPR difference image showing adsorption of human fibronectin (HFN) to patterned monolayer surfaces. (A) Difference image for the adsorption of 20 μg/mL HFN on ODT/MHA patterned surface. Brighter regions show HFN on MHA surface and darker regions indicate HFN on ODT monolayer film. (B) Difference image following HFN adsorption on ODT/MUL patterned substrate.

unfold and spread across the surface. Therefore, less protein per unit area would adsorb correlating to low signal intensity on the ODT region. The hydrophilic MHA surface denatures HFN to a lesser degree, hence greater amount of protein per unit area giving rise to the observed greater signal intensity on the MHA region. Therefore, we believe that the observed contrast in Figure 3.07A suggests different conformations/orientations for HFN on ODT and MHA monolayer surfaces.

Figure 3.07B indicates SPR difference image obtained from the adsorption of HFN on ODT/MUL patterned monolayer surface. The adsorption of HFN on the ODT/MUL patterned surface shows higher signal for HFN on ODT surface than on MUL as expected based on the IRRAS results in Chapter II. Based on the combined weight of our results from the IRRAS and SPR imaging, we can conclude that OH-terminated surfaces resist protein adsorption. Moreover, SPR imaging is capable of tracking differences in protein coverage as well as changes in the adsorbed state of the protein. SDS elution of HFN will be presented in the next section to further explore the capabilities of SPR imaging technique in tracking changes in adsorbed state of HFN.

SDS elution of HFN on ODT/MHA Patterned Substrate. This experiment was carried out the same way as the one presented in Figure 3.05. The result of SDS elution of HFN from the ODT/MHA patterned surface is presented in Figure 3.08. The cross-sectional profile for before and after SDS elution are also presented. Figure 3.08A represents the difference image of HFN adsorption

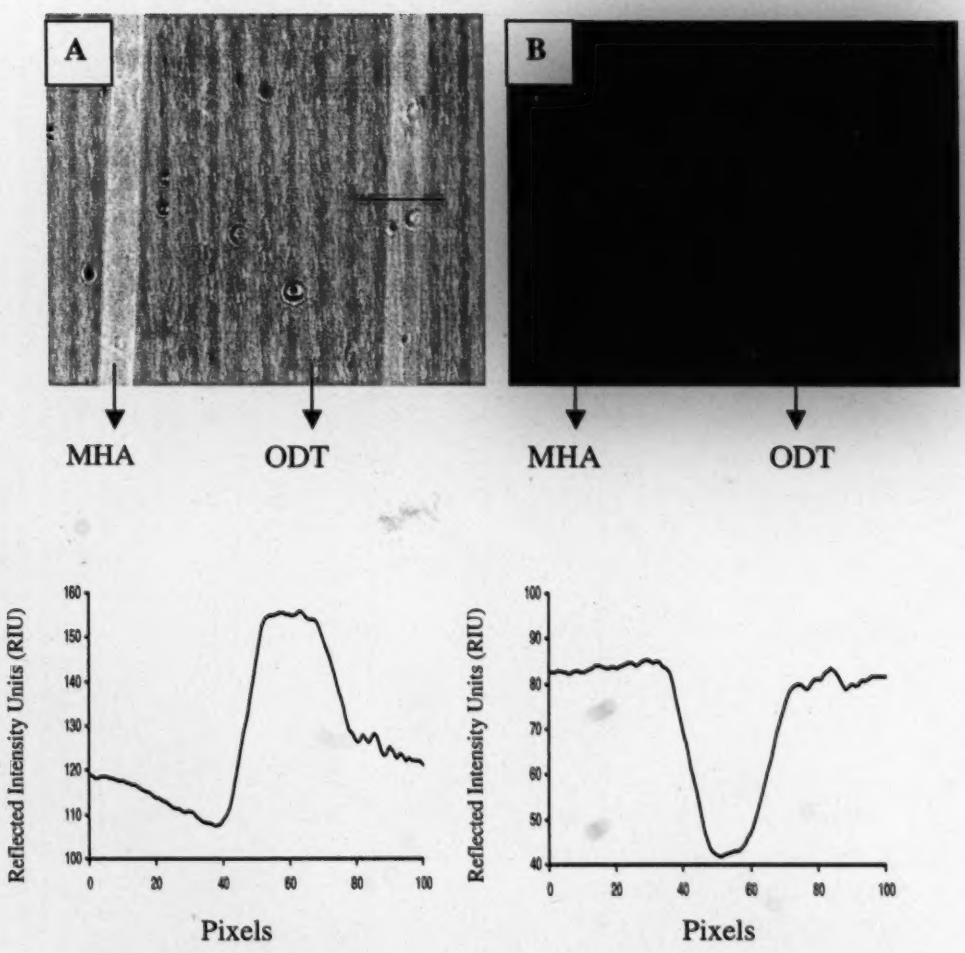

Figure 3.08. SPR difference images showing SDS elution of HFN on patterned gold substrates. (A) Before SDS elution of HFN on ODT/MHA patterned surface. Brighter regions indicate HFN adsorbed on MHA (COOH-terminated) monolayer surface and darker regions show HFN on ODT (CH_3-terminated) monolayer. (B) SPR image obtained after SDS elution of the image shown in (A). The change in contrast of image as observed in (B) is an indication of the removal of HFN by SDS. Lines shown in images A and B show the region cross-section profiles were taken.

before SDS elution. The effect of SDS elution of HFN is shown in Figure 3.08B. The darker contrast on MHA patterns indicates a much greater elutability of HFN compared to ODT surface.

Moreover, the cross-sectional profiles in Figure 3.08 shows a significant drop in measured intensity value on the MHA region after SDS elution compared to the ODT region. The amount of HFN eluted from the MHA regions is about four times that eluted from the ODT surface. In view of this, we believe that HFN adsorbs strongly to the ODT monolayer surface than the MHA monolayer. This contrast reflects differences in adsorbed HFN on MHA relative to ODT as observed above for HFG. The strong HFN-ODT hydrophobic interaction does not allow removal of significant amount of the surface-bound protein by SDS. This further confirms the conformational/orientation changes of adsorbed proteins associated with greater denaturation and decreased surfactant elutability [33]. We again employed antigen-antibody interactions to substantiate this claim.

Anti-HFN Binding to HFN. The interaction between fibronectin and anti-human fibronectin on ODT/MHA patterned surface was carried out to further probe the changes in protein conformation/orientation. Figure 3.09A. is the difference image showing HFN adsorption from 20 μg/mL solution. Figure 3.09B indicates the exposure of HFN film in Figure 3.09A to 105 μg/mL anti-HFN solution for 1 h. Brighter regions in both images indicate HFN and/or anti-HFN adsorption on MHA patterned surfaces. We observed a significant

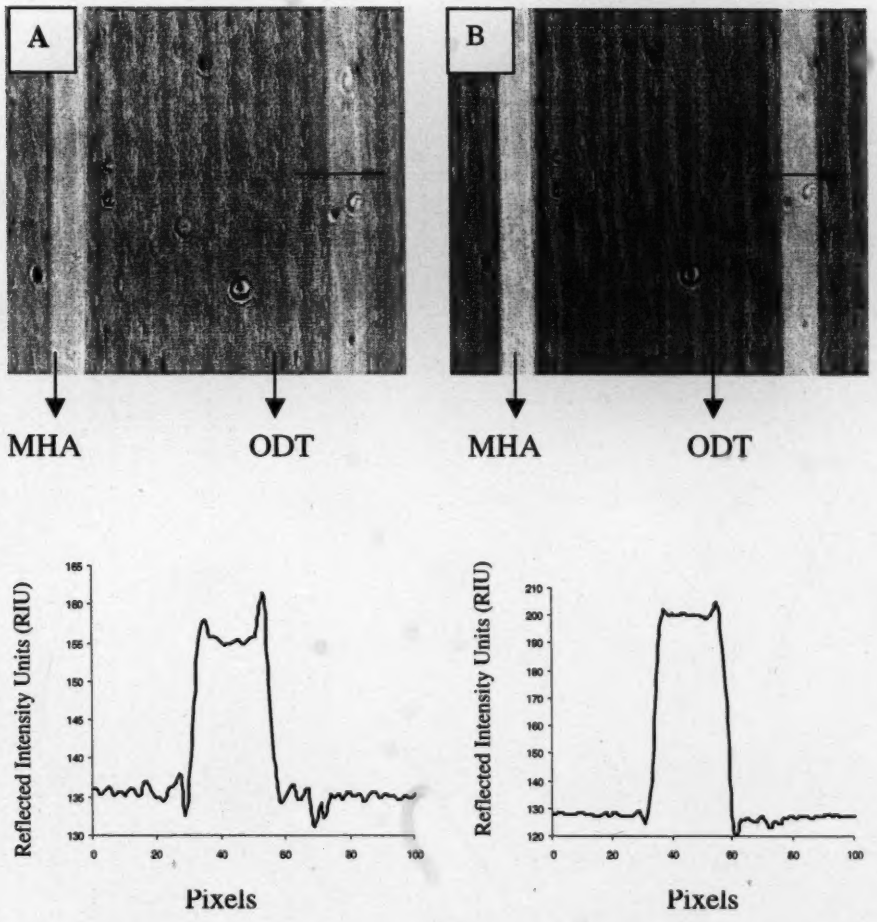

Figure 3.09. SPR difference images showing antibody binding to HFN adsorbed to patterned monolayers. (A) Difference image after the adsorption of 20 μg/mL HFN on ODT/MHA patterned surface. (B) Difference image after the exposure of adsorbed HFN to 105 μg/mL anti-HFN. Lines shown in images A and B show the region cross-section profiles were taken.

increase in intensity following adsorption of anti-HFN on the HFN/MHA region compared to the HFN/ODT region as indicated on the cross-sectional profile. The observed contrast following anti-HFN binding is believed to be due to differences in HFN conformation/orientation. On the HFN/MHA surface, HFN conformation/orientation exposed more binding sites or epitopes at the interfaces. No information on specific epitopes involved. However, evidence from the SDS elution results presented above does suggest that HFN adsorbed in a different state on MHA region compared to the ODT modified Au substrate. The results presented in this section show clearly that SPR imaging can be used to monitor protein interactions and qualitatively discriminate between surface-induced conformational/orientation changes of adsorbed proteins.

Conclusions

This chapter has demonstrated for the first time the ability of SPR imaging to monitor conformational/orientation changes of proteins on patterned monolayers on Au substrate. Antibody binding and surfactant elution studies further substantiated this claim. Chemically patterned monolayer surfaces, created by microcontact printing, generated contrast in SPR images. Variations in intensity profiles resulted from changes in index of refraction correlated to changes in adsorbed protein conformation/orientation. In the future, the protocols developed in this chapter could be used to investigate protein

interactions on patterned monolayers of protein resistant surfaces, such as glycols.

References

1. R. M. Corn and C. E. Jordan, Anal. Chem. 69:1449 (1997).
2. R. M. Corn, C. E. Jordan, A. G. Frutos, and A. J. Thiel, Anal. Chem. 69:4939 (1997).
3. R. M. Corn, B. P. Nelson, A. G. Frutos, and J. M. Brockman, Anal. Chem. 71:3928 (1999).
4. R. M. Corn, H. J. Lee, and T. T. Goodrich, Anal. Chem. 73:5525 (2001).
5. Y. Levy, P. Guedon, T. Livache, F. Martin, F. Lesbre, A. Roget, and G. Bidan, Anal. Chem. 72:6003 (2000).
6. J. M. Brockman, B. P. Nelson, and R. M. Corn, Annu. Rev. Phys. Chem. 51:41 (2000).
7. R. M. Corn, G. J. Wegner, and H. J. Lee, Anal. Chem. 74:5161 (2002).
8. L. A. Lyon, M. D. Musick, and M. J. Natan, Anal. Chem. 70:5177 (1998).
9. P. Schuck, Annu. Rev. Biophys. Biomol. Struct. 26:541 (1997).
10. I. O'Brien, M. J., V. H. Perez-Luna, S. R. J. Brueck, and G. P. Lopez, Biosensors and Bioelectronics 16:97 (2001).
11. G. B. Sigal, C. Bamdad, A. Barberis, J. Strominger, and G. M. Whitesides, Anal. Chem. 68:490 (1996).

12. G. B. Sigal, M. Mrksich, and G. M. Whitesides, Langmuir 13:2749 (1997).

13. G. M. Whitesides, R. E. Holmlin, X. Chen, R. G. Chapman, and S. Takayama, Langmuir 17:2841 (2001).

14. X. Chen, R. Ferrigno, J. Yang, and G. M. Whitesides, Langmuir 18:7009 (2002).

15. S. L. McGurk, R. J. Green, G. H. W. Sanders, M. C. Davies, C. J. Roberts, S. J. B. Tendler, and P. M. Williams, Langmuir 15:5139 (1999).

16. R. A. Frazier, M. C. Davies, G. Matthijs, C. J. Roberts, E. Schacht, S. J. B. Tendler, and P. M. Williams, Langmuir 13:7115 (1997).

17. F. E. Black, M. Hartshorne, M. C. Davies, C. J. Roberts, S. J. B. Tendler, P. M. Williams, and K. M. Shakesheff, Langmuir 15:3157 (1999).

18. T. Wink, J. de Beer, W. E. Hennink, A. Bult, and W. P. van Bennekom, Anal. Chem. 71:801 (1999).

19. J. L. Brash and T. A. Horbett, in Proteins at Interfaces II: Fundamentals and Applications (T. A. Horbett and J. L. Brash, eds.), American Chemical Society, Washington, D. C., 1995, p. 1.

20. T. A. Horbett and J. L. Brash, in Proteins at Interfaces: Physicochemical and Biochemical Studies (J. L. Brash and T. A. Horbett, eds.), American Chemical Society, Washington, DC, 1987, p. 1.

21. D. R. Lu and K. Park, J. Colloid Interface Sci. 144:271 (1991).

22. G. M. Whitesides and Y. Xia, Angew. Chem. Int. Ed. 37:550 (1998).

23. G. M. Whitesides, A. Kumar, and H. A. Biebuyck, Langmuir 10:1498 (1994).

24. G. M. Whitesides and A. Kumar, Appl. Phys. Lett. 63:2002 (1993).

25. G. M. Whitesides, Y. Xia, J. Tien, and D. Qin, Langmuir 12:4033 (1996).

26. B. D. Ratner, D. J. Graham, and D. D. Price, Langmuir 18:1518 (2002).

27. M. D. Porter, T. B. Bright, D. L. Allara, and C. E. D. Chidsey, J. Am. Chem. Soc. 109:3559 (1987).

28. M. D. Porter, T. B. Bright, D. L. Allara, and C. E. Chidsey, J. Am. Chem. Soc. 109:3559 (1987).

29. C. D. Bain, E. B. Troughton, Y.-T. Tao, J. Evall, G. M. Whitesides, and R. G. Nuzzo, J. Am. Chem. Soc. 111:321 (1989).

30. J. T. Woodward, M. L. Walker, C. W. Meuse, D. J. Vanderah, G. E. Poirier, and A. L. Plant, Langmuir 16:5347 (2000).

31. J. L. Bohnert and T. A. Horbett, Journal of Colloid and Interface Science 111:363 (1986).

32. T. J. Lenk, T. A. Horbett, B. D. Ratner, and K. K. Chittur, Langmuir 7:1755 (1991).

33. T. Arnebrant and M. C. Wahlgren, in Protein at Interfaces II: Fundamentals and Applications (T. A. Horbett and J. L. Brash, eds.), American Chemical Society, Washington, DC, 1995, p. 239.

34. B. D. Ratner, C. D. Tidwell, and S. I. Ertel, Langmuir 13:3404 (1997).

35. K. L. Egodage, B. S. de Silvia, and G. S. Wilson, J. Am. Chem. Soc. 119:5295 (1997).

CHAPTER IV

CONCLUSIONS AND FUTURE WORKS

Overall Conclusions

This research was aimed at probing in greater depth the adsorption characteristics of proteins, namely coverage and changes in conformation and/or orientation, onto modified gold substrates. The results presented in the preceding Chapters have demonstrated that infrared reflection absorption spectroscopy (IRRAS) and surface plasmon resonance (SPR) imaging are powerful diagnostic techniques for monitoring protein interaction at interfaces. Experimental results were presented to achieve the objectives set forth in Chapter I.

Over the past several years, many reports have appeared in which surfaces have been designed for specific protein interaction [1]. The ability to control specific and non-specific protein adsorption at interfaces would provide enormous contribution to understanding the complexity of protein interactions. In Chapter II, different surface chemistries were utilized to provide a platform to map variations in the amount of protein adsorbed and surface-induced protein conformations. These surfaces were characterized by IRRAS and contact angle measurement techniques. Octadecanethiol (ODT) presented a model neutral, hydrophobic $-CH_3$ surface. 16-mercaptodecanoic acid (MHA) provided a hydrophilic, partially negatively charged -COOH surface at pH 7.4. –OH terminated monolayers of 11-mercapto-1-undecanol (MUL) surfaces also manifested protein-resistant

capabilities. Polystyrene spin-coated and unmodified gold substrates presented hydrophobic and partially hydrophilic substrates respectively. Unmodified gold surface was found to be less hydrophilic under laboratory conditions. This resulted from adsorption of organics and other impurities in the atmosphere. The use of differing surface hydrophobicities tremendously influenced protein adsorption.

Application of IRRAS on single component monolayers demonstrated that fibrinogen (HFG), fibronectin (HFN), bovine serum albumin (BSA) and lysozyme (LYS) have different adsorption characteristics. Amide I band position was used as a diagnostic tool for the changes in conformation of adsorbed proteins. The adsorbed proteins showed significant peak shifts in amide I band positions to higher frequencies compared to those of the native protein. The shift in amide I band position was correlated to changes in conformation of the proteins upon adsorption onto solid substrates. Amide II band intensity, on the other hand, was used to track the amount of protein adsorbed to each surface. Fibrinogen, for example adsorbed significantly to all surfaces. This behavior of HFG confirmed the greater affinity of fibrinogen to different types of surfaces [1, 2]. However, it showed similar coverage on $-CH_3$ and –COOH terminated monolayers on gold. Human fibronectin exhibited no adsorption on the –OH terminated monolayer due to possible disruptions from water and solvent molecules. BSA was found to be the most hydrophilic protein. Antibody binding to fibrinogen was used to further probe the conformational changes of fibrinogen adsorbed on $-CH_3$ and –COOH terminated monolayers. Fibrinogen was because it showed similar coverage on

these surfaces. The antibody binding to fibrinogen revealed that fibrinogen exhibits different adsorbed states on the -CH_3 and –COOH monolayers, and this is due to the differences in the surface chemistries of the monolayers. The role of surface chemistry on protein adsorption was further explored in Chapter III.

Work presented in Chapter III demonstrated for the first time the ability of SPR imaging to map the differences in adsorption characteristics of HFG and HFN in low concentrations of 20 μg/mL. Chemically patterned monolayer surfaces of CH_3/COOH and CH_3/OH generated contrast in SPR images. HFG adsorbed more to COOH surfaces than CH_3 surfaces. The observed contrast on CH_3/COOH patterned surface following HFG adsorption was attributed to differences in the state of the adsorbed protein. This claim was supported by sodium dedocylsulfate (SDS) elution. HFG preferentially eluted from –COOH region relative to the CH_3 surface indicating different adsorbed conformations of HFG on both surfaces. Similar experiments were performed using HFN. Antibody binding to fibrinogen on CH_3/COOH provided further evidence for the conformational changes in adsorbed fibrinogen on each of the surface chemistries. Hence, the contrast in surface plasmon resonance images of the adsorbed proteins correlates to different adsorbed states of proteins at patterned substrates.

Suggestions for Future Works

SPR imaging results obtained in this research have demonstrated the ability of this technique in monitoring protein adsorption on patterned surfaces. However,

the adsorbed state of proteins on patterned monolayers would need further investigation. To further address the effect of surface chemistry on adsorbed state of a protein, there will be the need to pattern surfaces with poly(ethylene) glycol (PEG) that resist protein adsorption [3]. The chemistry of each of the adjacent microfabricated channels may be patterned with ODT, MHA and MUL monolayers. In this case, changes in protein conformation will be effectively assessed and a detailed quantitative information on the amount of the adsorbed protein will be obtained since PEG regions will serve as a baseline for measuring reflected intensity profiles. Such information will also help to evaluate the influence of surface chemistry on protein adsorption. Antibody binding and surfactant elution studies on such a substrate will also provide enough evidence on conformational changes. Different protein microarrays that allows analysis of several biological interactions in a single measurement can also be generated on this system [4, 5].

Further work is also required to explore the mechanisms of protein unfolding and quantification of the amount of protein adsorbed for the SPR imaging technique. The use of mass spectrometry will help determine exposed fragments of the adsorbed protein. Installation of a software package that produces the sensogram of the adsorption event will provide kinetic information as well as amount of protein adsorbed to surface. This information will be useful for detecting variations refractive index and to track changes in conformations.

It would also be interesting to use IRRAS to explore protein adsorption on mixed monolayers on Au. This would involve varying proportions of the individual components of the monolayer solution. Modified Au surfaces may be characterized using IRRAS and contact angle measurements. The later technique will serve as a diagnostic for surface hydrophobicity. Protein adsorption on such surfaces will help to further probe adsorption characteristics of protein.

References

1. J. L. Brash and T. A. Horbett, in Proteins at Interfaces II: Fundamentals and Applications (T. A. Horbett and J. L. Brash, eds.), American Chemical Society, Washington, D. C., 1995, p. 1.
2. K. Prime and G. M. Whitesides, Science 252:1164 (1991).
3. G. M. Whitesides, R. E. Holmlin, X. Chen, R. G. Chapman, and S. Takayama, Langmuir 17:2841 (2001).
4. R. M. Corn, H. J. Lee, and T. T. Goodrich, Anal. Chem. 73:5525 (2001).
5. R. M. Corn, G. J. Wegner, and H. J. Lee, Anal. Chem. 74:5161 (2002).